Institute of Freshwater Ecology

Institute of Freshwater Ecology

Transportation of pesticides by colloids

W A House PhD CChem FRSC
G P Irons PhD GRSC
B V Zhmud PhD

Report To: Department of the Environment
CEH Project No: T11059N2
IFE Report Ref.No: RL/T11059N2/14

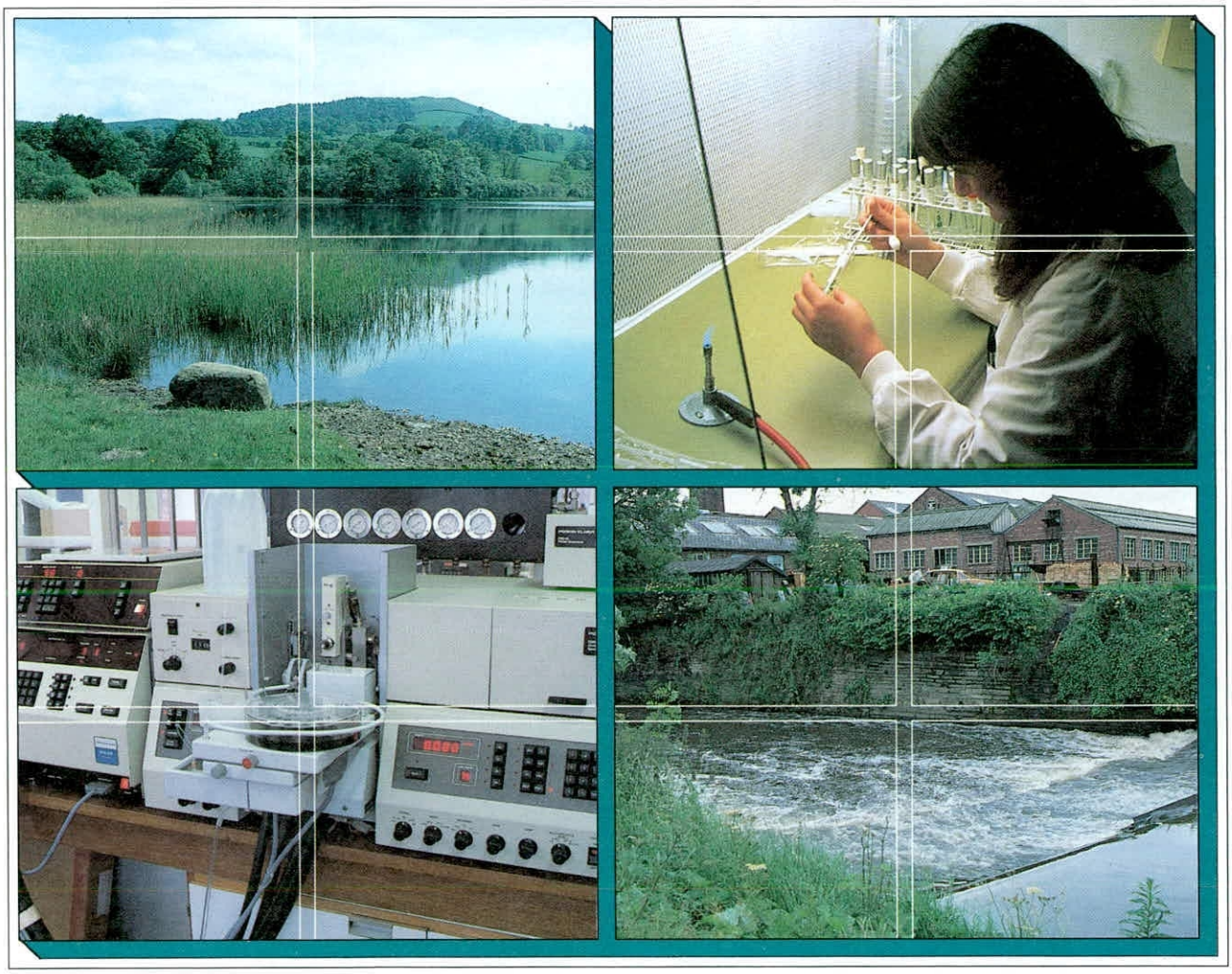

Centre for Ecology & Hydrology

Natural Environment Research Council

Institute of Freshwater Ecology

River Laboratory
East Stoke, Wareham
Dorset BH20 6BB
United Kingdom

Telephone +44 (0)1929 462314
Facsimile +44 (0)1929 462180
Email

TRANSPORTATION OF PESTICIDES BY COLLOIDS

W A House PhD CChem FRSC
G P Irons PhD GRSC
B V Zhmud PhD

Project Leader: W A House
Report Date: December 1996
Report To: Department of the Environment
CEH Project No: T11059N2
IFE Report Ref.No: RL/T11059N2/14

Centre for Ecology & Hydrology
Institute of Freshwater Ecology
Institute of Hydrology
Institute of Terrestrial Ecology
Institute of Virology & Environmental Microbiology

Natural Environment Research Council

INTELLECTUAL PROPERTY RIGHTS

CONFIDENTIALITY STATEMENT

'In accordance with our normal practice, this report is for the use only of the party to whom it is addressed, and no responsibility is accepted to any third party for the whole or any part of its contents. Neither the whole nor any part of this report or any reference thereto may be included in any published document, circular or statement, nor published or referred to in any way without our written approval of the form and context in which it may appear.'

CONTENTS

Summary

GLOSSARY

C_f: Concentration of pesticide in the filtrate
C_s: Concentration of pesticide in the supernatant
C: Concentration of colloids, mg l^{-1}
C_w: Concentration of pesticide in water in resin experiments
C: Concentration of suspended solids
CFC: Continuous-flow-centrifuge
DOC: Dissolved organic carbon
EtAc: Ethyl acetate
k_d: Distribution coefficient
K_b: Distribution coefficient for bottle in resin experiments
K_r: Distribution coefficient for resin
$L_{\pi c}$: Adsorption of pesticide to resin
NOM Natural organic matter
NPD: Nitrogen phosphorus detector (GC)
PTV: Programmable temperature vapouriser injector (GC)
SFE: Supercritical fluid extraction
spe: Solid-phase extraction
SS: Suspended sediment
UFC: Ultrafiltration cell

SUMMARY

Progress of the project between June 1996 and December 1996 is reported. The work covers adsorption studies on clay colloids, characterisation of sediments isolated by continuos-flow centrifugation from the Humber rivers and further trials to investigate the performance of resins in competitive adsorption with pesticides.

The adsorption of flutriafol to kaolinite, montmorillonite and silica is shown to be dominated by hydrogen bonding and hydration effects. The measured Henry constants (a measure of the affinity of the compound to the surface) are similar for the three colloids. The calculated distribution coefficients are much smaller than the values measured for the DOC. The results also indicate that flutriafol does not interact with the interlayers of montmorillonite and only with the edge sites of the clay. Both isoproturon and propiconazole interact weakly with the mineral colloids and give distribution coefficients similar to those measured for environmental samples.

The characterisation of the suspended sediments from the rivers Aire, Swale and Ouse, isolated by continuos-flow-centrifugation, indicate that the major part of the sediment occurs in the silt between 2-63 μm in size with negligible material greater than 900 μm in diameter. The clay contents are generally less than 12 % by volume, although sedimentation results produce much higher values by mass (31-35%). Mineral analysis shows the occurrence of a range of clays including kaolinite, montmorillonite and illite with feldspars as relatively minor components. In the mineral fraction, e.g. as isolated by filtration with 0.45 μm membrane, it is difficult to separate the finer particulates and colloids from the larger size fraction in quantity sufficient for pesticide analysis. A more productive approach is to characterise the minerals isolated by filtration to find the lower size cut-off and treat the smaller macromolecules which penetrate through these filters using different techniques, e.g. by using ultrafiltration methods.

The competitive adsorption method, which appeared promising in the last report, proved to be unsuccessful. Recent results have indicated an attachment of the colloids to the resins and difficulties in the analysis of the pesticide concentrations. Although the method still has potential, there is no further time to develop this approach in this project. Hence all future work will use the ultrafiltration method developed in the first 18 months of the project.

1.0 Introduction

The majority of contaminants entering surface waters and discharging to the sea, regardless of their source, do not remain dissolved in the water but become adsorbed onto suspended solids and may at some stage sediment out. They may also be associated with colloids which are unlikely to sediment out. Consequently, movement of most contaminants from the source of inputs is a complex process and is a only loosely related to major water movement patterns. Understanding the movement and partitioning of contaminants is important in assessing their impact in surface waters and loading to the sea.

The project seeks to improve the understanding of the role of colloids in the long-range transportation of contaminants, and in particular of pesticides, both in riverine movement to estuaries, where colloids are likely to flocculate, and dispersion in near coastal waters.

2.0 Programme of work

The first two years are planned as follows:

1. Development of an automated ultrafiltration unit with low molecular weight cut-off (500-10000 Daltons) for sorption measurements.

2. Measurement of the sorption affinity of pesticides using the adsorption cell with 0.01 μm membrane filter, to enable some comparisons with the ultrafiltration experiments containing the smaller colloids. Initial tests with XAD resins will also be carried out at this stage.

3. Test the performance of the ultrafiltration unit in experiments without a membrane and also in experiments with a membrane but without colloids present.

4. Measure sorption isotherms in freshwater conditions and over a range of pH.

5. Measure isotherms to determine the affinity of the pesticides to the colloids in solutions of different salinity.

Items 1-3 are expected to be completed in the first year and 4-5 in the second year.

3.0 Progress to date

The development of the automated ultrafiltration cell was described in the report (RL/T11059n1-3). This included the construction of parts of the system, interfacing the valves and ancillary equipment to a computer and testing the performance. The development of the control software was also outlined in the last report.

Research has also continued in the following areas:

(a) The analysis of natural waters from the Humber rivers to ascertain the importance of colloids in the transportation of selected pesticides. The research has used the ultrafiltration cell (UFC) developed in the project.
(b) Characterisation of natural suspended sediments and colloid fractions in the rivers Ouse, Aire, and Swale in Yorkshire.
(c) Adsorption isotherm measurements and theoretical interpretation.
(d) Development of a competitive adsorption method using DAX-8 resin.

This report covers the items (b) to (d) above.

4.0 Characterisation of natural suspended sediments

4.1 Methods

Samples of river water (50 litre as "whole water" samples), were collected from selected Humber rivers (Aire, Ouse and Swale). Some of these waters have been used in ultrafiltration experiments

described in previous reports. In addition to these, samples were collected in February and June 1996 for characterisation.

In summary the methods used are as follows:

(a) Determination of the particle-size distribution by sedimentation

This follows the operating procedure: IFE SOP 26/20.7.94. The method was run without the addition of a deflocculation agent.

(b) Determination of the particle-size distribution by Laser granulometry.

This was done using a Coulter LS130 laser instrument to measure sizes in the range of 0.1 to 900 μm. The sample was suspended in tap water containing a small amount of dispersant and continually pumped through the cell. A beam of monochromatic light of wavelength 750 nm is used in the instrument to form a 13 mm diameter beam passing through the sample cell. Light is diffracted by particles to an angle which is dependant on their size. The smaller the particle, the larger the angle of diffraction. The diffracted light passes through a Fourier lens to focus on a 126 photodiode detector. The lens ensures that the diffracted light is focused at a specific angle for that particle size independently of the position of the particles in the cell. The intensity of light at each detector is measured and the Fraunhofer model is used to determine the particle size distribution.

(c) The mineral composition of the suspended and colloidal sediment was measured by X-ray diffraction using a Philips PW 1380 horizontal goniometer with 1710 diffraction control. Measurements were made on the whole water sediment samples and also the clay fractions (i.e. < 2 μm in diameter).

4.2 Results

4.2.1 Particle-size distributions

The results from laser granulometry are summarised in Table 1 for all the samples. The results for the samples collected from the R. Ouse, R. Swale (16.9.94) and R. Aire (13.12.95) are compared with those obtained by sedimentation in Table 2. The two sites on the R. Swale are at Catterick and about 57 km south at Crakehill near the confluence of the Swale with the Ure and Ouse. Both sites are adjacent to the Environmental Agency (EA) gauging stations. Typical river bank material was also collected from a site in the middle of the reach between Catterick and Crakehill near the village of Maunby. The R. Swale, in this section south of Catterick, is particularly susceptible to bank erosion during storm periods. The other two sites on the rivers Aire and Ouse are close to the EA gauging stations at the inter-tidal limits. The site at Naburn on the Ouse is south of York and the main STW input from York. The results show:

a) The suspended solids in these rivers is mainly in the size classification of 2-63 μm, i.e. the silt fraction.
b) The suspended solids from the rivers Aire and Ouse had low sand contents. In contrast, the R. Swale sediment contained more sand, probably as a results of the contributions from bank erosion.

This is demonstrated from the results of the analysis of the river bank material from Maunby on the river Swale as shown in Table 1. The bank material contains approximately equal proportions of the sand and silt fractions.

c) There is negligible suspended material greater than 900 μm in size.

d) The clay contents of the suspended material is generally less than 12 % by volume by laser granulometry. However, the results in Table 2 indicate substantial differences between the laser granulometry and sedimentation results for the clay fraction (< 2 μm). For the rivers Aire and Ouse, the clay fraction amounts to 35 and 31 % by mass compared with 10 and 11 % by volume by laser granulometry. This implies that the particulates in this fraction are of high density and compact rather than low density organic material.

e) Apart from the river bank material, the particle-size distributions (see Appendix 1), are all similar with medians between 10 and 20 μm. The R. Swale sediments do show some evidence of multiple peaks; for example the peak between 100 and 200 μm found in the sample collected from Crakehill on 1.5.96 is coincident with the second peak in the distribution of the river bank material.

4.2.2 Mineral characterisation

A brief introduction to the colloidal clay minerals and terminology is given below:

a) Kaolinite group. These are 1:1 type minerals composed of alternate tetrahedral silica and octahedral aluminium sheets producing a layer thickness of about 0.7 nm. Members of the group include kaolinite, dickite, nacrite, serpentine and halloysite. The particles are usually 0.05-5 μm in size with a relatively low specific surface area (10-30 $m^2 g^{-1}$) and cation exchange capacity of 3-15 meq per 100g.

b) 2:1 type minerals (2 tetrahedral silicas and 1 octahedral aluminium sheet). These includes the expandable minerals (smectites) such as montmorillonite and vermiculities.and also non-expanding fine-grained micas (illite). The smectite group is noted for interlayer expansion which is a result of swelling when wetted. Montmorillonite is the predominant member of this group although beidellite, nontronite and saponite are also found in soils. There is strong evidence that some polar pestcides can penetrate the interlayer spacing of the expandable clays and so become less labile. In illite, K^+ ions of low hydration, usually balance the charge and produce a non-expanding mica layer of approximately 1.0 nm, whereas in vermiculite, containing hydrated Mg^{2+} ions, the interlayer spacing is 0.498 nm corresponding to a bilayer of water between the sheets. The cation exchange capacity of montmorillonites are much greater than non-expanding minerals, usually in the range of 80-150 meq per 100 g of clay with specific surface areas of 70- 100 $m^2 g^{-1}$. Illite differs from micas in that the stacking of layers of illite is more random than mica, the particles are finer than in mica, small amounts of Ca and Mg are present in the interlayer of illites but not in micas and aluminium substitution in the tetrahedral sheets is much less than in true mica.

c) Chlorites are iron-magnesium silicates with some aluminium present. Typically, 2: 1 layers such as in the smectites, alternate with Mg-dominated trioctahedral sheets. Mg also dominates the trioctahedral sheets in the 2:1 layer and so the crystal contains two silica tetrahedral sheets and two Mg-dominated trioctahedral sheets.

d) Feldspars are mainly in two groups: alkali feldspars and plagioclase feldspars. The former includes K-feldspar ($KAlSi_3O_8$). The plagioclase feldspars comprise the series between $NaAlSi_3O_8$ and $CaAl_2Si_2O_8$. They are both similar in structure to the polymorphs of SiO_2, consisting of an infinite network of SiO_4 as well as AlO_4 tetrahedra. The structure can be considered as a derivative

of SiO_2 structures, by incorporation of Al into the tetrahedral network, and concomitant housing of Na^+ (or K^+ or Ca^{2+}) in available voids.

The whole sediment analysis revealed the presence of quartz (sand or silica) and mica in all the samples. Kaolinite was found to be a dominant mineral present in many samples. Calcite, was measured in trace quantities in all the rivers. Vivianite (see Table 3) is an iron phosphate ($Fe_3(PO4)_2$. $8H_2O$) mineral which is a weathering product of Fe-Mn-phosphates and rarely encountered in rivers. The clay analysis, Table 4, indicates the dominance of illite and kaolinite in all the samples. The clays from the river bank material (R. Swale) were similar in composition to the suspended sediment from that river. The expandable clays (an illite-smectite mixture) were also important in these rivers.

The LOIS special topic project on the Humber rivers (Pesticide Interactions with Sediments) has also found similar minerals in the river bed-sediments (< 5 cm depth). Smectites and illite were the dominant clay minerals with kaolinite being important for the rivers Calder and Don. These results are based on one years quarterly sampling of bed-sediments. The results for the suspended sediments are not yet available. One feature of the characteristics of the sediments is the difference between the surface areas of the suspended sediments and colloids and the bed-material (< 5 cm depth). The annual mean specific surface area (measured by nitrogen adsorption and BET analysis) of the bed- sediments from the rivers Ouse, Aire, Swale, Calder, Don and Trent were 4.7, 5.7, 4.1, 5.1, 5.0 and 6.1 $m^2\ g^{-1}$ compared with 8.3, 9.5, 6.8, 8.0, 10.7 and 13.1 $m^2\ g^{-1}$ for the suspended material isolated by continuous-flow-centrifugation.

5.0 Adsorption isotherm measurements

The adsorption of flutriafol, propiconazol and isoproturon have been measured at 20 ^0C on silica, kaolinite and montmorillonite clays at pH=7. The two clays were prepared by the methods given in Appendix 2. These silicates were chosen because of their occurrence in the Humber rivers (and rivers in general). Initial studies with a ground quartz material failed because of the difficulties of measuring isotherms with limited available surface area of adsorbent exposed to the solution. Instead, a high specific area silica gel was used to determine the adsorption affinity to compare with the two clay minerals. Silica also acted as a model material to investigate the interactions with the edge sites of the clays and feldspars.

Adsorption isotherms were measured using the batch method with the suspensions prepared in $KHCO_3$ solution and pH adjusted to 7 with CO_2 / N_2 gas mixture. Initial studies with kaolinite were made using an adsorption cell similar to the design of the ultra-filtration equipment (UFC) but with filtration by a syringe pump rather than by N_2 pressure. This apparatus was also used to measure the kinetics of the sorption interaction of the pesticides with the minerals.

The adsorption isotherms are shown in Figure 1, 2 and 3. These indicate the amount of pesticide associated with the silicates (in $\mu g\ g^{-1}$ (dry weight of clay)) at different solution concentrations. The adsorption is linear with no signs of saturation of the surface with the compounds. Additional experiments also showed that the compounds did not compete for adsorption sites, i.e. the density of sorption sites on the minerals is much greater than the surface

density of the pesticides. This is supported by the abeyance to Henry's law (the limiting form of the Langmiur equation):

$$n_a = \Sigma.w.T.\ c \qquad [1]$$

where n_a is the adsorption amount in μg of pesticide, Σ is the specific surface area in $m^2\ g^{-1}$, w is the mass of the colloid, T is the Henry's law constant (in m) and c the equilibrium concentration of pesticide in the solution (μg dm^{-3}). The Henry constant is related to the adsorption energy of the pesticide to the clay by:

$$T = \int_0^\infty [\exp(-U / kT) - 1] ds \qquad [2]$$

where U is the interaction energy with the surface and s the surface area.
The Henry constant is related to the distribution coefficient by:

$$K_d = T\ \Sigma.\ 10^6 \quad dm^3\ g^{-1} \qquad [3]$$

The results of the calculation of the Henry's constants are shown in Table 5 for the three adsorbents and three pesticides. A discussion of the results for flutriafol is given in Appendix 2 together with the results of the chemical modelling of the interaction of specific functional groups of the compound with clay surfaces. The adsorption affinity of flutriafol changes in the sequence montmorillonite> kaolinite> silica gel. Molecular interactions indicate a weak interaction of the flutriafol with the clay which is dominated by hydration and hydrogen bonding effects. It is also possible that the triazole base interacts with the acidic bridged hydroxyls by the acid-base mechanism. The main factor determining the adsorption affinity is: (i) competition of flutriafol with water molecules in the surface layers of the clay, (ii) competition of functional groups on flutriafol with water molecules in the hydration sphere of cations and (iii) protonation of the base in the surface layers of the clay and adsorption of the compound in cationic form. The small difference in the Henry's constant for kaolinite and montmorillonite suggest that penetration of flutriafol into the interlayers of montmorillonite is not an important mechanism in the time scale of the experiments. The molecular calculations using MOPAC (Molecular Orbital Package) indicate that the bonding energy of water to the silanol (i.e. -SiOH surface) is close to that of flutriafol.

6.0 Development of a competitive adsorption method

During the period leading up to this report the methods used for the physical manipulation of the samples during the extractions were refined.

6.1 Method

A volume of sample was shaken in PTFE bottles with a quantity of resin (DAX-8) selected to reduce the concentration of pesticides present by approximately half. After 24 h incubation at 10°C the contents of the bottles were poured into 70 ml reservoirs and any resin not transferred rinsed in to the reservoir with water out of the reservoir. The samples were then drawn through

an empty 3 mm glass column fitted with a PTFE frit, which captures the resin, and a solid-phase extraction cartridge which had been pre-conditioned in the normal manner.

The pesticides isolated by the solid-phase extraction were eluted and prepared for GC analysis. Initially the columns were extracted using the normal procedure for a solid-phase extraction cartridge but it was found impossible to adequately control the elution rate, therefore the following modified elution procedure was adopted. A drying column, containing anhydrous sodium sulphate, was placed on a vacuum manifold with a valve and needle leading to a 2 ml collection vial. The glass column containing the resin was fitted on top of this, and 2 ml of ethyl acetate (EtAc) pipetted into it. The elution of the liquid was started, and about 1 ml of EtAc was drawn down out of the glass column. At this point the extraction was stopped using the valve, and an unused solid-phase extraction cartridge fitted to the top of the glass column. The extra air resistance provided by the extraction cartridge enables the extraction to continue in a controlled manner, and the extract to be collected efficiently. In the absence of the cartridge, extract is usually lost from the vials as a result of the high air flow through the resin

6.2 Introduction to experimental work.

The compounds studied were the same as in the previous UFC studies. Some problems were encountered in adequate resolution of the some of the compounds by GC(NPD) and these have been omitted from the report. The pesticides reported are: simazine, atrazine, propazine, terbutryn, fenitrothion, malathion and parathion.

A series of experiments were performed to study the influence of specific effects on the competitive adsorption method. These included experiments to confirm that the bottles did not significantly adsorb the pesticides. Measurements of the distribution of pesticide between the resin and the aqueous phase, (based on measurements of pesticides extracted from the resin rather than lost from solution). Initial tests were also performed with water from the R. Aire at Beale, and comparisons made with solutions containing Aldrich Humic acid.

6.3 Measurement of adsorption to containers.

Fourteen bottles containing various dilutions of stock pesticide solution were incubated for 24 h. Eight measurements were made of the concentration of the stock, and the average of these values used to obtain predicted concentrations for each of the bottles. The concentrations measured in the bottles after 24 h was plotted against the expected concentration, and regression statistics obtained. Distribution coefficients (K_b = amount adsorbed by bottle / concentration in solution or amount adsorbed by bottle per dm^2 / concentration in solution), were calculated from the regression gradients where possible and are summarised below. In a separate experiment eleven bottles were incubated for various times and the loss of pesticide was plotted as a function of time. It was noted that the bottles had reached equilibrium in under 24 h. Although these distribution coefficients appear small, there is significant loss of the compounds to the PTFE bottles amounting to 20-30 % at low concentrations.

	unit	Propazine	Parathion
K_b	dm^3/bottle	0.005	0.008
Standard error of K_b	dm^3/bottle	0.004	0.005
K_b	dm^3/dm^2	0.009	0.015
Standard error of K_b	dm^3/dm^2	0.007	0.009
Predicted recovery	%	89	83

6.4 Confirmation of resin sorption properties

6.4.1 Adsorption kinetics on the resin

The initial experiments (report TL/T11059N2/3) estimated the distribution of the pesticide (K_d) from the loss of pesticide measured in solution. The final method will rely on direct measurements of the pesticide sorbed on the resin, by extraction of the pesticides. The kinetics of the adoption of the selected pesticides onto the resin DAX-8 was therefore reinvestigated. Twelve bottles were prepared each containing a known mass or pre-wetted resin. A fixed volume (50 ml) of stock pesticide solution (10 $\mu g\ l^{-1}$ nominal) was pipetted into each bottle, and incubated at 10°C for various time before being separated and extracted as described above. Two additional bottles were treated in the same way except that their contents were shaken and then immediately separated without incubation.

After GC (NPD) analysis, the adsorption on the resin samples were calculated (amount of pesticide extracted / dry mass resin) and the concentrations in the water samples calculated (amount of pesticide extracted / volume water). The distribution coefficient for the resin in each bottle, (K_r), was then calculated and plotted against contact time. It was noted that all the pesticides showed a rapid rise in distribution coefficient prior to the first measurement. The distribution coefficients became unmeasurable after 48 h for all the pesticides because the concentrations in the aqueous phase dropped below the limit of determination of the method. It was also noted that although none of the pesticides appear to have reached adsorption equilibrium, simazine, atrazine, propazine and parathion appeared to be further from equilibrium than fenitrothion and malathion. For experimental convenience it was decided to set the incubation time at 24 h. Using linear fits to the kinetic data, the effect of uncertainty in the measurement of incubation time was assessed giving the values summarised below. In practice it has been found that the incubation time may be fixed at 24 h ± 15 min.

Percentage error in into estimate of distribution coefficient associated with incubation for 24 ± 1 hours

	Simazine	Atrazine	Propazine	Fenitrothion	Malathion	Parathion
Distribution coefficient	2996	3083	11861	1808	6949	14554
% error	17	16	17	8	15	17

6.4.2 Resin isotherms

The above estimates of the distribution coefficient after 24 h mixing were refined using a series of 10 bottles containing known masses of resin. Various dilutions of a stock (10 μg l^{-1} nominal) pesticide solution were pipetted into the bottles which were incubated at 10°C for 24 h. After 24 h the contents of the bottles were separated, extracted and the extracts analysed. In a separate experiment over a week later two bottles were prepared, incubated and analysed in the same manner to check that the results obtained were reproducible. The adsorption on the resin were plotted against the concentrations in solution for each pesticide where more than 3 valid points were obtained in the main experiment - many points could not be plotted as the concentration of pesticide in the solution had dropped below the limit of determination. The plots for the three remaining pesticides (simazine atrazine and parathion) showed a large degree of scatter superimposed upon the expected trend of a straight line through the origin. Regression analysis was performed for a model line through the origin for the two sets of data separately. The results are summarised in the table below. It was noted that there was no significant difference (95% confidence limit) between the two sets of estimates which were then pooled to obtain the third estimate values of K_r listed below.

	simazine	atrazine	parathion
K_r	1784	2962	23616
standard error of K_r	200	530	2692
Degrees freedom	6	4	4
K_r(2nd week)	1389	2483	22988
K_r (2nd week)	160	304	5425
Degrees freedom	1	1	1
Third estimate K_r	1727	2866	23490
pooled standard error	195	493	3418
Coefficient variation, CV %	11	17	15

6.5 Method tests

6.5.1 Initial test with a natural water from the R. Aire.

Four bottles containing known masses of resin, and various mixtures of filtered water from the R. Aire, (collected on 24.10.95 from the R. Aire at Beale, NGRSE534255) and stock pesticide solution. (ratios: 9:1, 3:2, 2:3, 1:9) were incubated with the bottles used to measure the Kr and separated, extracted and analysed in the same way. In both of these bottles the proportion of the pesticides remaining in the liquid was increased suggesting that the method can detect the binding of pesticides by the colloids present in this natural water. Net distribution constants for simazine and atrazine were calculated for the colloids naturally occurring in the R.Aire water using the equation:

$$K_{dc}=10^6*[(C_w \cdot K_{dr}/ L_{rc})-1]/C \qquad (4)$$

where C is the concentration of DOC in mg l^{-1}, C_w is the concentration of pesticides present in the water from the bottle in $\mu g\ l^{-1}$, K_{dr} is the distribution constant for the resin in $dm^3\ kg^{-1}$ and L_{rc} is the adsorption of pesticide on the resin in $\mu g\ kg^{-1}$. The results are summarised below:

Example	bottle 1	bottle 2	UFC measurement (Table 3: Report: RL/T11059N2)
DOC concentration / mg dm^{-3}	2.19	8.76	21.9
simazine, K_d / $dm^3\ g^{-1}$	186	32	9.5
atrazine, K_d / $dm^3\ g^{-1}$	256	78	11.8

It may be noted that the values estimated by the competitive adsorption method are higher than those measured by the ultrafiltration cell (UFC). Unfortunately the experiments with the bottles with the highest DOC concentration used with the competitive adsorption method were unsuccessful because the extracts were accidentally spilled. The two results shown for the competitive method with low DOC concentrations indicate a dependence of K_d, on the DOC concentration. This is very unlikely unless the DOC was partitioned in some way prior to dilution so that the bottles contained different size distributions of the colloids. It is more likely that the uncertainties in the measurement of the pesticides are such that the results shown are unreliable. The uncertainties are:

(a) There is some interaction between the resin and the colloid. Any tendency for the colloidal material to attach itself to the resin beads will result in a lowering of the K_d value obtained with this effect being more significant at higher concentrations of colloid. If the variation is due to colloid resin interactions, then either the separation procedure would have to be modified to remove the colloid from the surface of the resin before extraction of either phase, or a number of experiments would have to be performed on each water and a more complex model fitted to the data in order to estimate the extent of each interaction.

(b) An alternative explanation could be that the as the concentration of colloids is reduced below that found in the natural water (and used in the UFC) experiment, interactions within the colloidal fraction are reduced and as a result the colloids present a greater surface area to the water. If this is the case then either additional experiments are required to quantify these effects, or all measurements will have to be performed using the natural concentration of colloids, i.e. without significant dilution or pre-concentration.

Values are not available for the other pesticides due to a combination of a lack of suitable K_d values for the pesticides on the resin, and the appearance of negative results for many of the substances as a result of uncertainty in the analytical measurements. Data has been collected but requires further processing before it can be used to estimate the other K_d values.

6.5.2 Tests with Aldrich humic acid

Ten bottles containing known masses of resin, various quantities of water and stock humic acid solution (100 mg dm^{-3} Aldrich Humic acid, sodium salt) together with 50 ml of stock pesticide solution (10 μg dm^{-3} nominal) to give 10 different humic acid concentrations in the range 0 - 10 mg dm^{-3} and a constant amount of pesticides in each bottle. These bottles were then incubated for 24 h, before being separated, extracted and analysed. Initially eqtn. 1 was used to calculate the distribution of pesticide between the water and the humic acid (using the amount on the resin to predict the concentration of pesticide "free" in the water and obtaining the amount on the humic acid by subtraction). The results from this model were found to be variably, producing K_d values fluctuating around zero. No trend in the K_d's was found with increasing concentration of humic acid. The poor results are largely due to problems in the analytical method resulting in higher than normal scatter in the measured concentrations of the pesticides. The method relies on the determination of a difference between two quantities, i.e. the concentration of "free" pesticide predicted from the adsorption to the resin and the concentration in the solution containing colloids. Hence absolute errors in the individual measurements are added to produce the absolute error in the amount adsorbed to the colloid. If the latter is small, the percentage error in the adsorption amount becomes excessive.

7.0 UFC results- final K_d's

The results shown in Table 6 have been calculated from the data previously presented in interim reports using the results from the DOC analysis to give the K_d's normalised with respect to organic carbon. The previous results were estimated from preliminary DOC measurements or DOC values obtained from the uv/vis absorbance.

8.0 Further work

The next stage of the project is to estimate the pesticides associated with the colloid component which are transported in one of the Humber rivers and complete the experiments on the sorption of selected pesticides on colloid material examining the effects of temperature and ionic strength. In view of the lack of progress with the competitive adsorption method, the ultrafiltration cell (UFC) method will be used to estimate colloid partition with DOC. The pesticides selected for study will probably include those often measured in the R. Aire, e.g. simazine, carbaryl and diazinon. Parathion and flutriafol will also be included to cover a range of chemical properties. It is planned the research will be done as follows:

1. Samples from the R. Aire (at the intertidal limit) will be taken on a weekly or fortnightly basis. They will be characterised by measurement of pH, dissolved oxygen, temperature, conductivity, suspended solids, DOC and uv/vis absorption. Pesticides will be measured by the method employed in the LOIS project, i.e solid-phase extraction (spe) with retention of suspended and colloid sediments and separate elution of the sediment and spe columns. The sediments will be retained for particle-size analysis. Colloids passing through the extraction column will be measured by filtration through membranes of different size.

2. A further sample of the R. Aire water, pre-filtered through GF/F microfibre pad, will be used in the UFC after spiking with selected pesticides. The partition of the pesticides with the colloid component will be estimated using the procedure reported previously, RL/T11059N2. The DOC concentration in the filtrate and supernatant will be measured as well as the uv/vis characteristics. As many samples as possible will be analysed to enable a range of flow conditions, and hence suspended solids concentrations, in the river to be studied.

3. The temperature and ionic strength dependence of the adsorption of selected compounds including flutriafol, will be measured and modelled using a molecular approach. The ionic strengths studied will be from 0.01 to 0.6 M (as NaCl) to cover the transition from freshwaters to seawater. The measurement of the temperature dependence of the Henry's law constant will permit a comparison between the calculated and experimental enthalpy of adsorption and provide more information on the adsorption mechanism. Experiments with the UFC with the ionic strength increased to 0.6 M will enable the effects of ionic strength on the adsorption by DOC to be evaluated.

4. The analytical results (together with river discharge data from the EA) will be used to estimate the contribution of colloids in the transport of the selected compounds to the inter-tidal zone. The results from (1 and 2) will permit an estimate of the colloid bound load of simazine from DOC LOIS data obtained for the R. Aire from the autumn of 1993 to December 1996.

TABLE 1. Particle-size determination (% by volume) by laser granulometry for river suspended sediments isolated by continuous-flow centrifugation. The size-fractions are: < 2 μm, clay; 2-63 μm, silt; 63-2000 μm, sand. The size distribution of a river bank material collected form an eroded section of the R. Swale is also shown.

River	Site reference	Date	<2 μm	2-63 μm	63-900 μm	> 900 μm
Aire	Beale NGR: SE534255	21.6.96	5.55	90.36	4.09	0.0
Aire	Beale NGR: SE534255	13.12.95	10.07	85.92	4.01	0.0
Ouse	Naburn Lock NGR: SE594445	2.3.95	9.61	85.75	4.64	0.0
Swale	Catterick NGR: SE225994	16.9.94	10.66	76.16	13.18	0.0
Swale	Catterick NGR: SE225994	28.2.96	7.92	76.92	15.16	0.0
Swale	Crakehill NGR: SE425733	28.2.96	11.05	81.50	7.45	0.0
Swale	Catterick NGR: SE225994	1.5.96	5.49	71.84	22.67	0.0
Swale	Crakehill NGR: SE425733	1.5.96	6.88	72.48	20.64	0.01
Swale	Maunby bank material NGR: SE347862	28.2.96	7.82	45.50	46.68	0.0

TABLE 2

Comparison of the results for the particle-size determination by laser granulometry and sedimentation. KEY to methods: lg: laser granulometry (% by volume) and s: sedimentation (% by mass).

Site	Date	>20 μm	5-20 μm	2-5 μm	<2 μm
Ouse, Naburn (lg)	2.3.95	27	48	14	11
Ouse, Naburn (s)	2.3.95	9	42	17	31
Swale, Catterick (lg)	16.9.94	40	34	14	12
Swale, Catterick (s)	16.9.94	40	34	6	21
Aire, Beale (lg)	13.12.95	27	48	15	10
Aire, Beale (s)	13.12.95	10	31	24	35

TABLE 3. Qualitative whole sample analysis by X-ray diffraction. The minerals present have been ranked as dominant (D), present (P) and trace (T).

River	Date	mica	kaolinite	chlorite	quartz	K-feldspar	Plag. feldspar	calcite/ dolomite	vivianite
Aire, Beale	21.6.96	P			P			T	D
Aire, Beale	13.12.95	D	D		P	T	P		
Ouse, Naburn	2.3.95	P	D		D	T	T	T	
Swale, Catterick	16.9.94	P	D		P		T		
Swale, Catterick	28.2.96	P		D	D				
Swale, Crakehill	28.2.96	P	D		D		T	T	
Swale, Catterick	1.5.96	P	D		P			T	
Swale, Crakehill	1.5.96	P	D		P				

TABLE 4.
Semi-quantitative analysis of the clay fractions by X-ray diffraction (%). The expandable mineral is an illite-smectite mixed-layer of approximately equal proportions. Values of zero indicate a mineral is not identified as present.

River	Date	illite	expandable	kaolinite	chlorite
Aire, Beale	21.6.96	40	19	32	9
Aire, Beale	13.12.95	55	14	28	3
Ouse, Naburn	2.3.95	41	19	35	5
Swale, Catterick	16.9.94	44	18	35	3
Swale, Catterick	28.2.96	45	9	45	1
Swale, Crakehill	28.2.96	43	13	37	7
Swale, Catterick	1.5.96	49	4	47	0
Swale, Crakehill	1.5.96	45	15	40	0

TABLE 5.
Henry's law constants for adsorption of selected pesticides on silica gel, kaolinite and montmorillonite at 20 ^{0}C.

Colloid	Pesticide	Henry's constant/10^{-8} m	K_d/ dm^3 kg^{-1}
silica gel	isoproturon	9.1	27.3
300 m^2 g^{-1}	propiconazol	23	69.0
	flutriafol	2.9	8.7
kaolinite	isoproturon	26	2.5
9.5 m^2 g^{-1}	propiconazol	13	1.2
	flutriafol	8.7	0.8
montmorillonite	isoproturon	14	64.7
462 m^2 g^{-1}	propiconazol	66	304.9
	flutriafol	14	64.7

TABLE 6

Summary of the K_d values (in $dm^3\ g^{-1}$) that have been measured for river waters. The distribution coefficients are normalised with respect to the dissolved organic carbon values (DOC) measured or estimated from the visible absorbance at 340 nm. The sample: Aire(2), was not pre-filtered. KEY: CFC: continuous-flow centrifugation; GF/F: filtration with glass micro-fibre pad.

	R. Ouse	R. Ouse	R. Swale	R. Aire(1)	R. Aire(2)
Sampling date	2.3.95	2.3.95	16.9.94	24.10.95	24.10.95
Preparation	CFC	CFC	CFC	GF/F	none
membrane.	1000	10,000	1000	1000	1000
DOC/mg l^{-1}	4.86	7.90	17.5	21.9	15.3
simazine	19	1.1	5.3	9.5	12.4
atrazine	122	3.0	6.2	11.8	17.3
propazine	160	5.2	9.9	11.4	20.7
desmetryn	105	5.0	10.5	8.2	11.0
prometryn	150	-	32.9	6.4	5.4
terbutryn	-	33	8.5	6.1	-
fenitrothion	160	-	35.1	7.1	25.6
malathion	-	-	36.0	-	74.9
cyanazine	153	-	25.5	24.5	32.6
parathion	51	21	77	3.6	10.6

FIGURE 1.

Results of the adsorption measurements of isoproturon, flutriafol and propiconazol at 20 ^{0}C on kaolinite. The adsorption is measured as μg of pesticide on unit dry mass of clay. C_{eq} is the concentration of the pesticide measured after about 24 h contact with the clay.

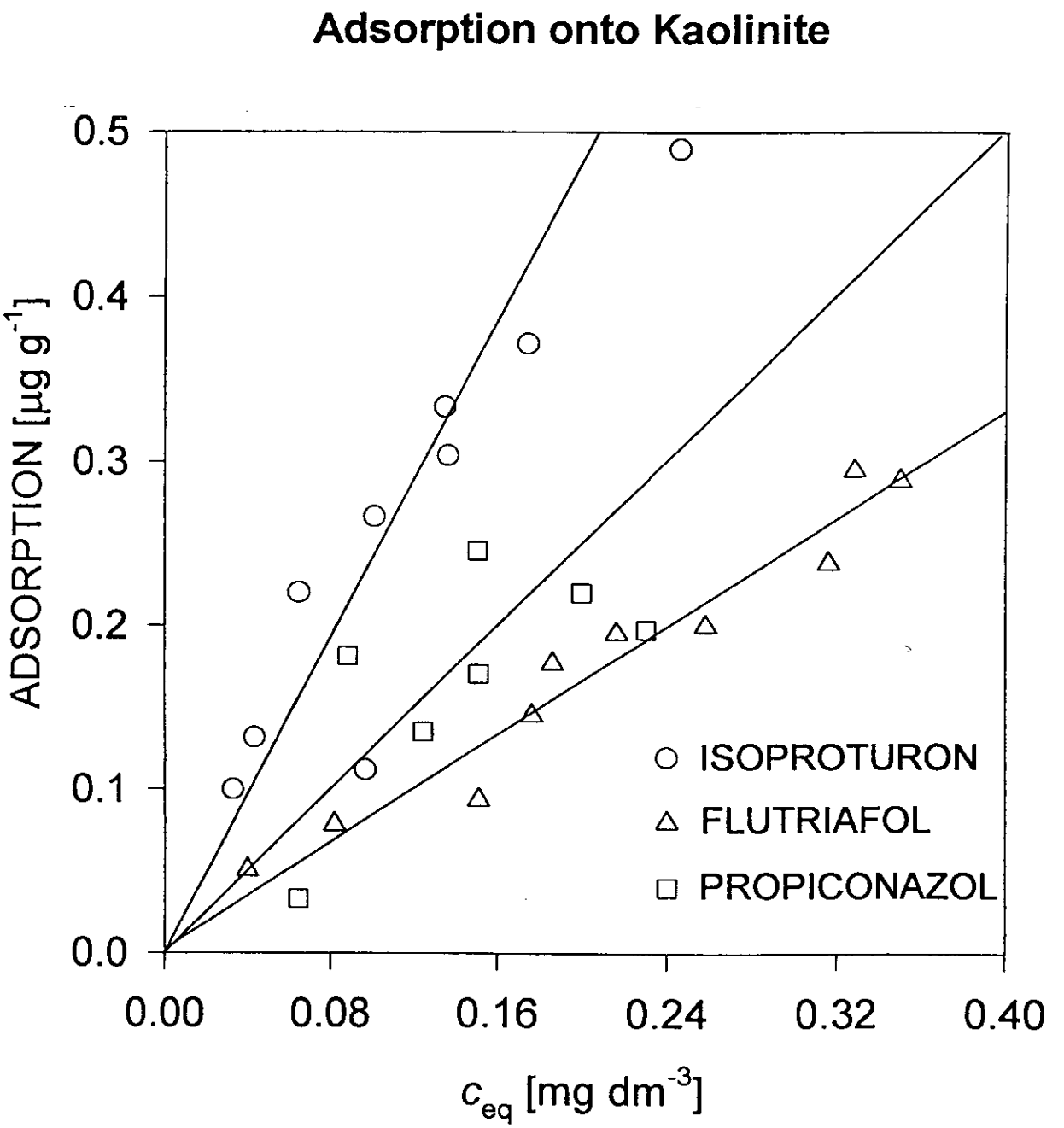

FIGURE 2.

Results of the adsorption measurements of isoproturon, flutriafol and propiconazol at 20 ^{0}C on silica gel. The adsorption is measured as μg of pesticide on unit dry mass of silicate. C_{eq} is the concentration of the pesticide measured after about 24 h contact with the clay.

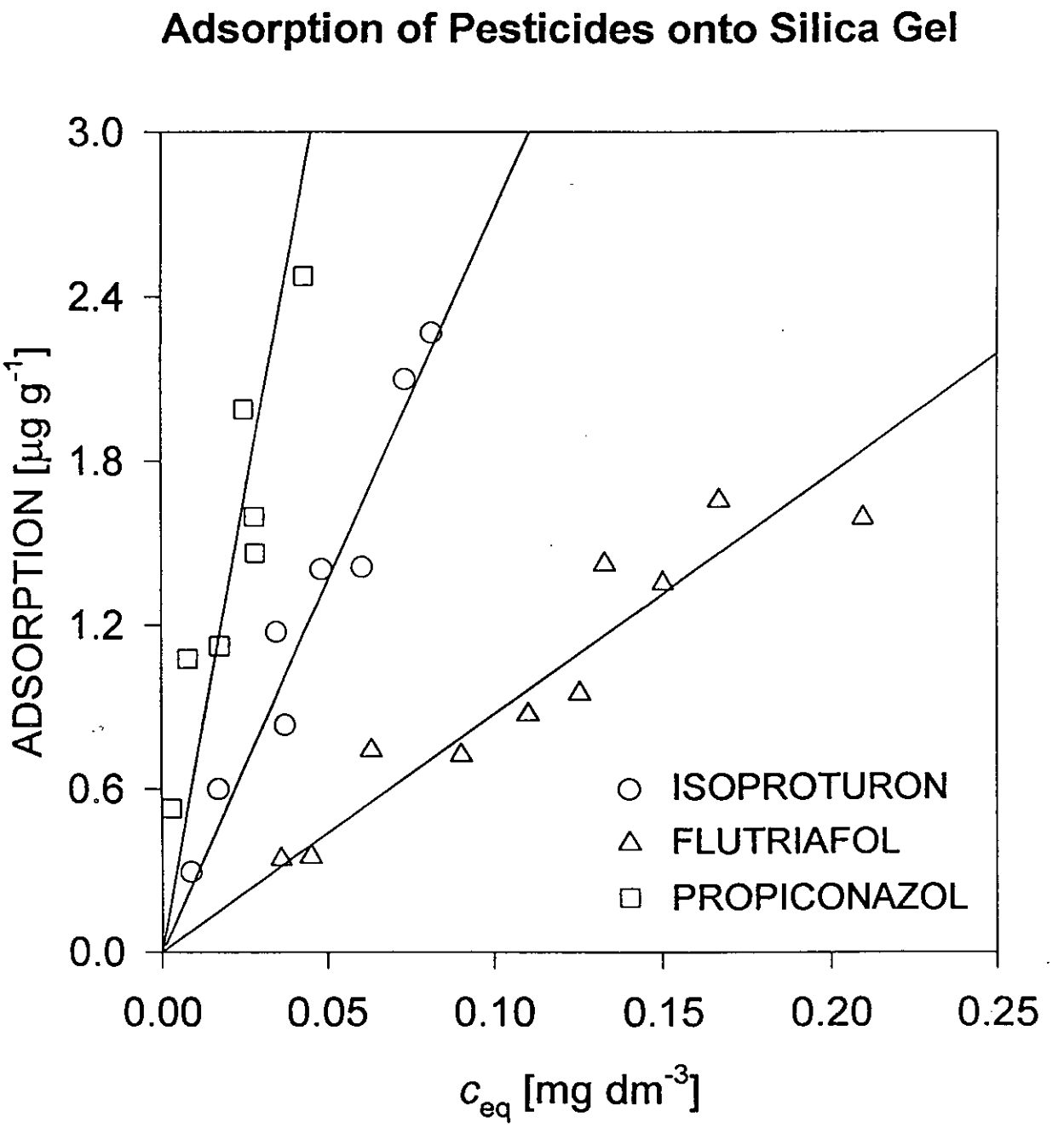

FIGURE 3.

Results of the adsorption measurements of isoproturon, flutriafol and propiconazol at 20 ^{0}C on montmorillonite. The adsorption is measured as μg of pesticide on unit dry mass of clay. C_{eq} is the concentration of the pesticide measured after about 24 h contact with the clay.

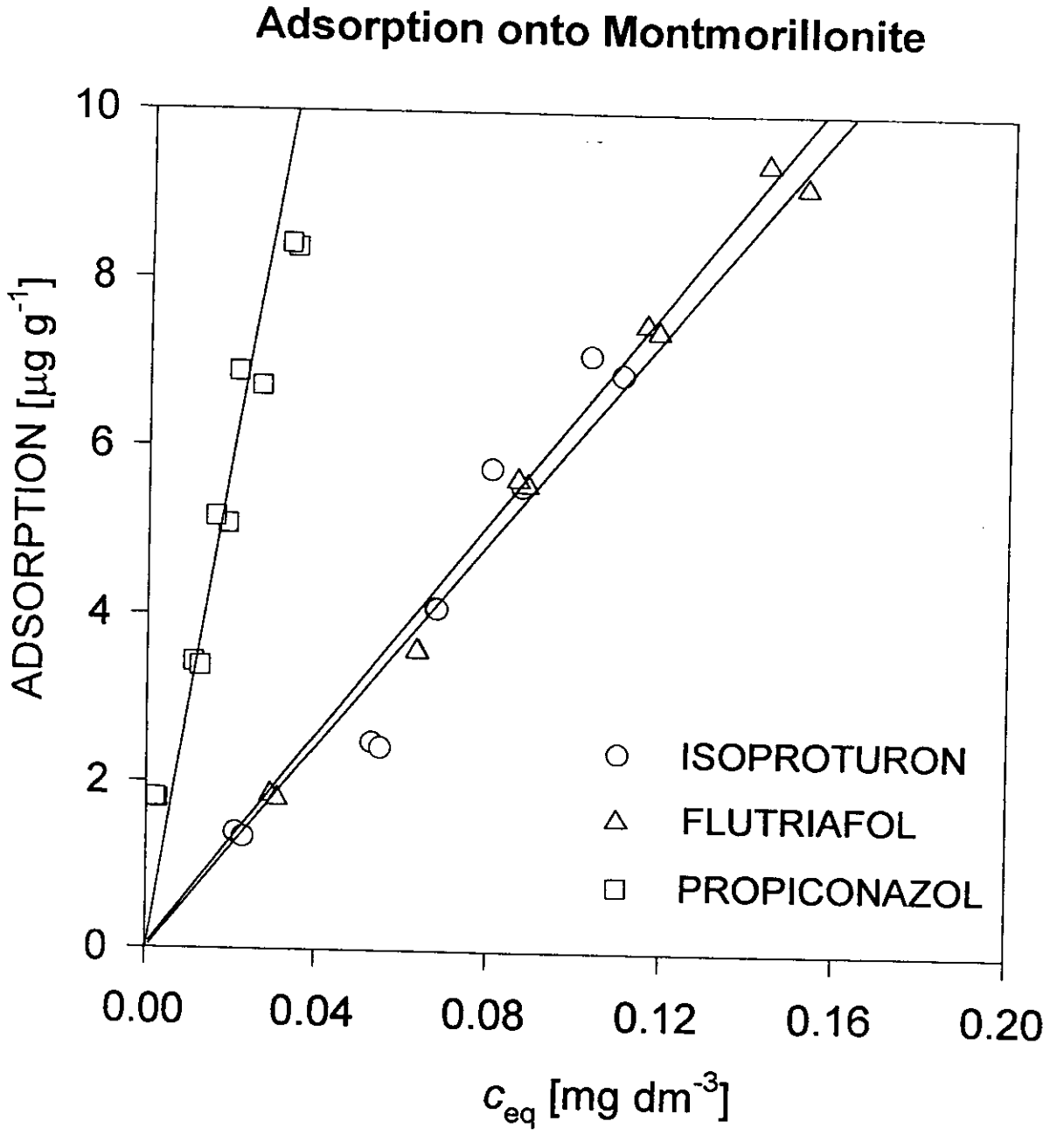

Appendix 1.

Particle-size distribution for suspended material collected from the Humber rivers.

R. Swale at Catterick on 16.9.94

freshec.$06

File name:	FRESHEC.$06	Group ID:	FRESHEC
Sample ID:	S1.9	Run number:	18
Operator:	DMT		
Comments:	DISPERSED IN CALGON		
Start time:	16:08 6 Sep 1996	Run length:	61 Seconds
Pump Speed:	48		
Obscuration:	11%		
Optical model:	Fraunhofer		
LS 130	Fluid module		
Software:	1.50	Firmware:	1.3 1.8

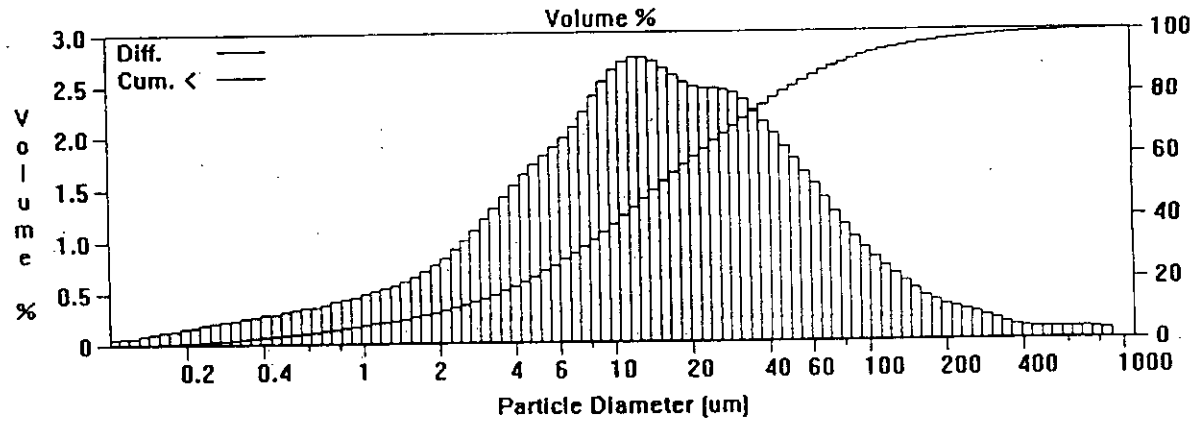

Volume Statistics (Arithmetic) freshec.$06

Calculations from 0.10 um to 900.00 um

Volume	100.0%		
Mean:	35.76 um	95% Conf. Limits:	21.10-50.43 um
Median:	14.09 um	Std. Dev.:	74.82 um
Mean/Median Ratio:	2.538	Variance:	5598 um^2
Mode:	13.05 um	Coef. Var.:	209.2%
		Skewness:	6.002 Right skewed
		Kurtosis:	46.50 Leptokurtic

% >	5.000	16.00	50.00	84.00	95.00
Size um	130.5	53.23	14.09	3.236	0.810

R. Swale at Catterick on 1.5.96

freshec.$01

File name:	freshec.$01	Group ID:	FRESHEC
Sample ID:	S10496.1	Run number:	13
Operator:	DMT		
Comments:	DISPERSED IN CALGON		
Start time:	14:31 6 Sep 1996	Run length:	60 Seconds
Pump Speed:	48		
Obscuration:	5%		
Optical model:	Fraunhofer		
LS 130	Fluid module		
Software:	1.50	Firmware:	1.3 1.8

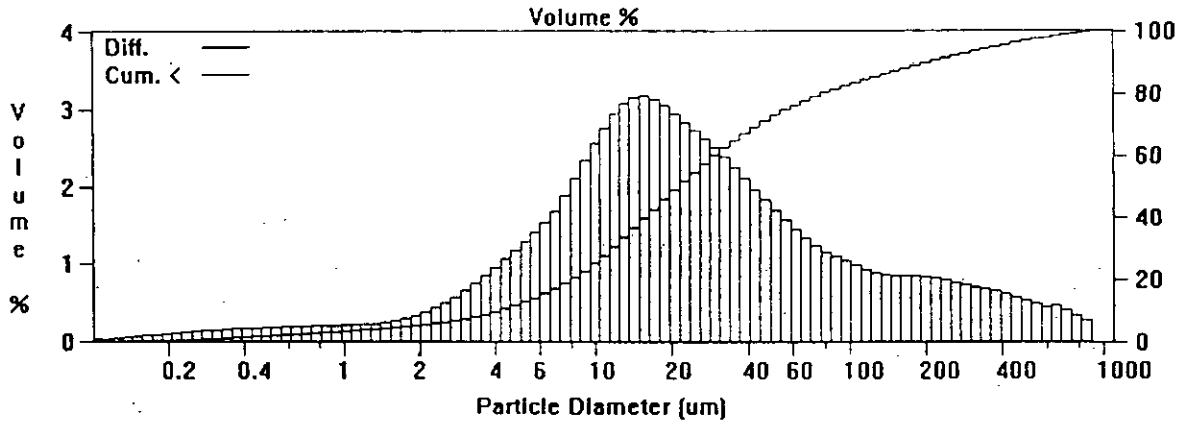

Volume Statistics (Arithmetic) freshec.$01

Calculations from 0.10 um to 900.00 um

Volume	100.0%		
Mean:	69.16 um	95% Conf. Limits:	43.46-94.85 um
Median:	20.35 um	Std. Dev.:	131.1 um
Mean/Median Ratio:	3.398	Variance:	17187 um^2
Mode:	15.65 um	Coef. Var.:	189.6%
		Skewness:	3.344 Right skewed
		Kurtosis:	12.18 Leptokurtic

% >	5.000	16.00	50.00	84.00	95.00
Size um	355.7	105.3	20.35	6.184	1.741

R. Swale at Crakehill on 1.5.96

File name:	FRESHEC.$04	Group ID:	FRESHEC
Sample ID:	S20496.2 CRAKEHILL	Run number:	16
Operator:	DMT		
Comments:	DISPERSED IN CALGON		
Start time:	15:43 6 Sep 1996	Run length:	60 Seconds
Pump Speed:	48		
Obscuration:	6%		
Optical model:	Fraunhofer		
LS 130	Fluid module		
Software:	1.50	Firmware:	1.3 1.8

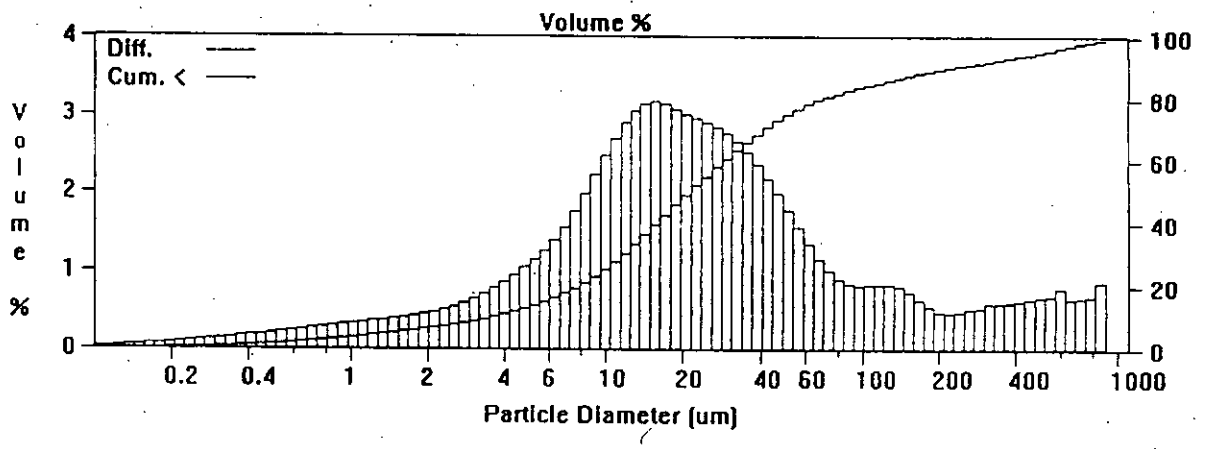

Volume Statistics (Arithmetic) freshec.$04

Calculations from 0.10 um to 900.00 um

Volume	100.0%		
Mean:	76.64 um	95% Conf. Limits:	45.73-107.5 um
Median:	20.28 um	Std. Dev.:	157.7 um
Mean/Median Ratio:	3.778	Variance:	24869 um^2
Mode:	15.65 um	Coef. Var.:	205.8%
		Skewness:	3.224 Right skewed
		Kurtosis:	10.23 Leptokurtic

% >	5.000	16.00	50.00	84.00	95.00
Size um	470.9	96.22	20.28	5.830	1.320

R.Swale at Maunby (river bank material) on 28.2.96

File name:	freshec.$02	Group ID:	FRESHEC
Sample ID:	BANK CORE 3ft	Run number:	14
Operator:	DMT		
Comments:	DISPERSED IN CALGON		
Start time:	14:42 6 Sep 1996	Run length:	60 Seconds
Pump Speed:	48		
Obscuration:	10%		
Optical model:	Fraunhofer		
LS 130	Fluid module		
Software:	1.50	Firmware:	1.3 1.8

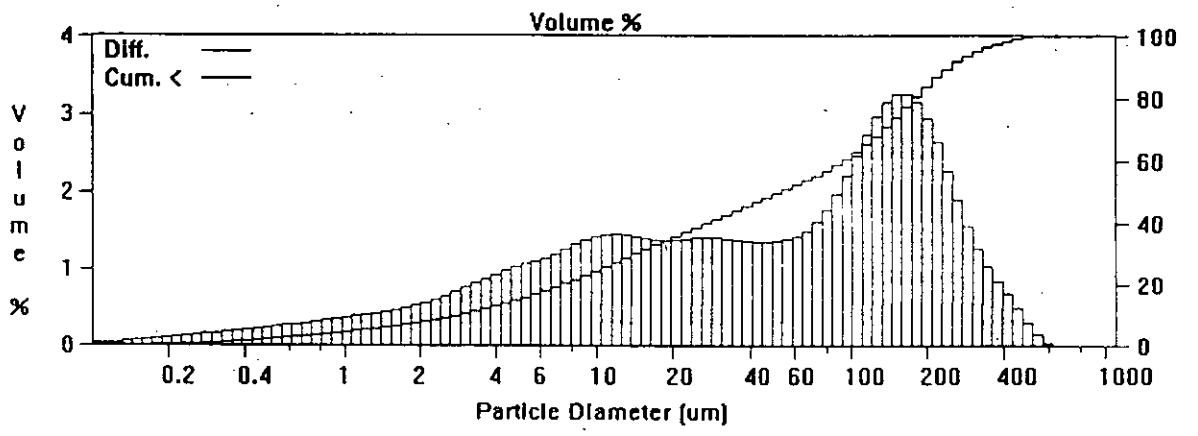

Volume Statistics (Arithmetic) freshec.$02

Calculations from 0.10 um to 900.00 um

Volume	100.0%		
Mean:	92.18 um	95% Conf. Limits:	72.03-112.3 um
Median:	50.38 um	Std. Dev.:	102.8 um
Mean/Median Ratio:	1.830	Variance:	10572 um^2
Mode:	167.0 um	Coef. Var.:	111.5%
		Skewness:	1.418 Right skewed
		Kurtosis:	1.906 Leptokurtic

% >	5.000	16.00	50.00	84.00	95.00
Size um	299.1	192.5	50.38	5.102	1.139

R. Swale at Crakehill on 28.2.96

File name:	FRESHEC.$10	Group ID:	FRESHEC
Sample ID:	S20296.5	Run number:	5
Operator:	DMT		
Comments:	DISPERSED IN CALGON	Run length:	61 Seconds
Start time:	11:54 9 Sep 1996		
Pump Speed:	48		
Obscuration:	11%		
Optical model:	Fraunhofer		
LS 130	Fluid module	Firmware:	1.3 1.8
Software:	1.50		

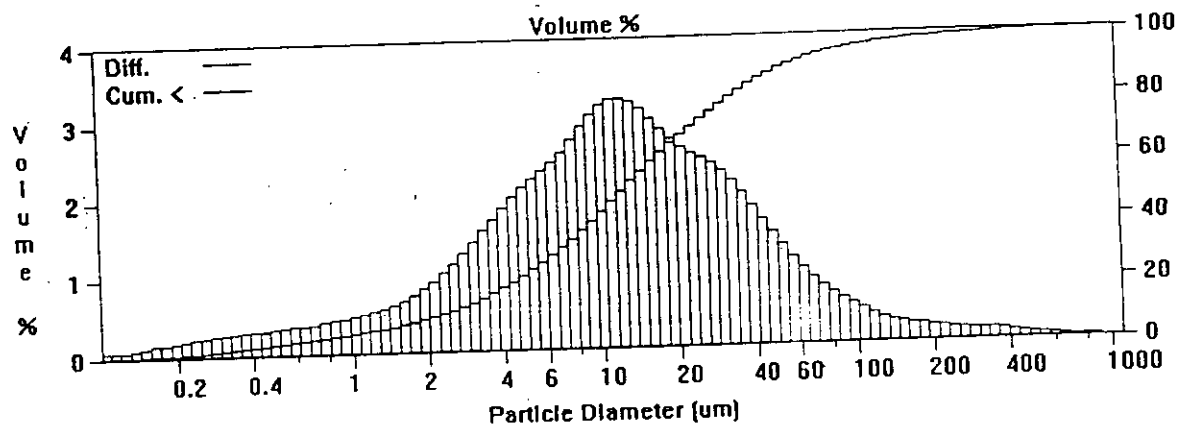

Volume Statistics (Arithmetic) freshec.$10

Calculations from 0.10 um to 900.00 um

Volume	100.0%		
Mean:	25.18 um	95% Conf. Limits:	14.63-35.73 um
Median:	11.26 um	Std. Dev.:	53.85 um
Mean/Median Ratio:	2.236	Variance:	2899 um^2
Mode:	11.91 um	Coef. Var.:	213.8%
		Skewness:	7.169 Right skewed
		Kurtosis:	70.00 Leptokurtic

% >	5.000	16.00	50.00	84.00	95.00
Size um	83.14	36.21	11.26	3.016	0.741

R. Swale at Catterick on 28.2.96

freshec.$09

File name:	FRESHEC.909	Group ID:	FRESHEC
Sample ID:	S10296.4	Run number:	4
Operator:	DMT		
Comments:	DISPERSED IN CALGON		
Start time:	11:35 9 Sep 1996	Run length:	60 Seconds
Pump Speed:	48		
Obscuration:	5%		
Optical model:	Fraunhofer		
LS 130	Fluid module		
Software:	1.50	Firmware:	1.3 1.8

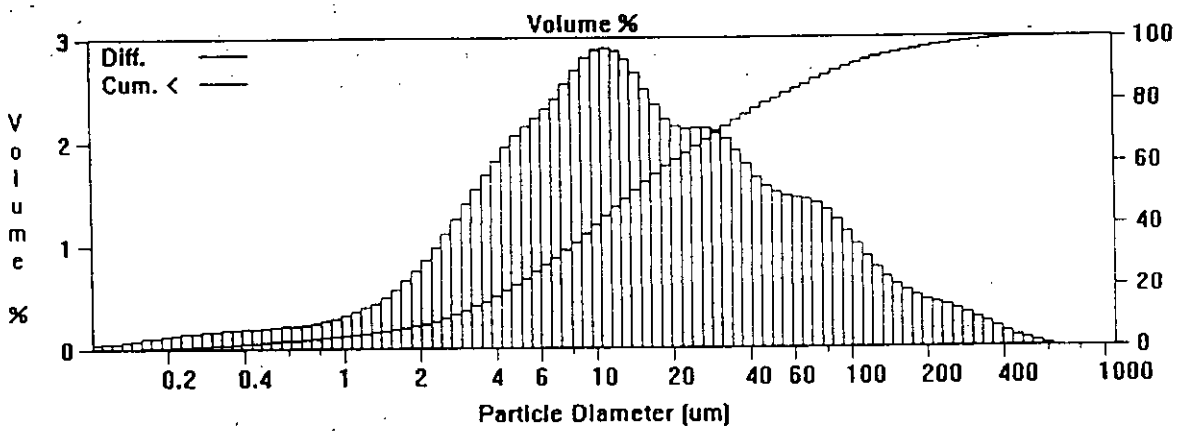

Volume Statistics (Arithmetic) freshec.$09

Calculations from 0.10 um to 900.00 um

Volume	100.0%		
Mean:	34.72 um	95% Conf. Limits:	23.03-46.40 um
Median:	13.07 um	Std. Dev.:	59.63 um
Mean/Median Ratio:	2.657	Variance:	3556 um^2
Mode:	10.88 um	Coef. Var.:	171.8%
		Skewness:	3.919 Right skewed
		Kurtosis:	20.04 Leptokurtic

% >	5.000	16.00	50.00	84.00	95.00
Size um	142.3	59.34	13.07	3.650	1.260

R. Ouse at Naburn on 2.3.95

freshec.$08

File name:	FRESHEC.908	Group ID:	FRESHEC
Sample ID:	Ou.7	Run number:	3
Operator:	DMT		
Comments:	DISPERSED IN CALGON		
Start time:	11:00 9 Sep 1996	Run length:	60 Seconds
Pump Speed:	48		
Obscuration:	11%		
Optical model:	Fraunhofer		
LS 130	Fluid module		
Software:	1.50	Firmware:	1.3 1.8

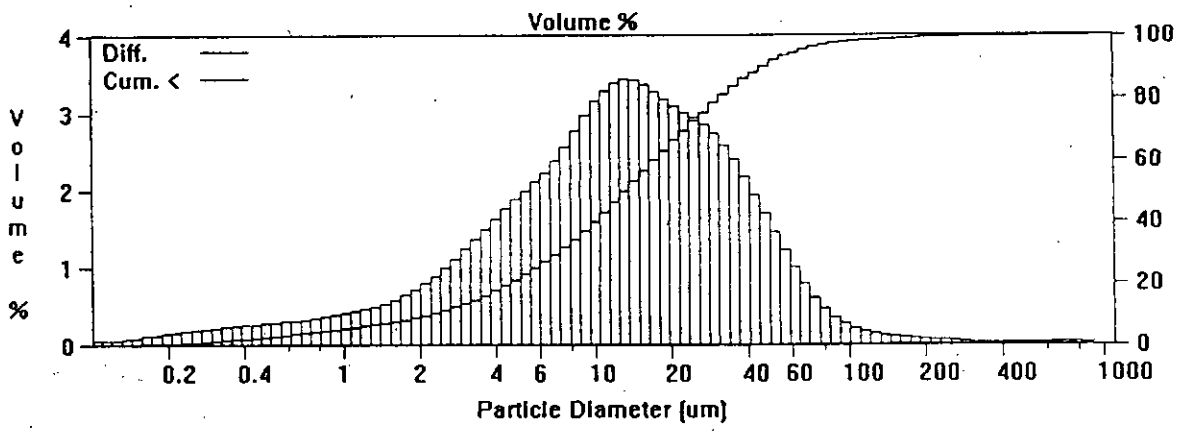

Volume Statistics (Arithmetic) freshec.$08

Calculations from 0.10 um to 900.00 um

Volume	100.0%		
Mean:	22.19 um	95% Conf. Limits:	13.05-31.33 um
Median:	12.56 um	Std. Dev.:	46.63 um
Mean/Median Ratio:	1.766	Variance:	2174 um^2
Mode:	13.05 um	Coef. Var.:	210.2%
		Skewness:	10.59 Right skewed
		Kurtosis:	146.0 Leptokurtic

% >	5.000	16.00	50.00	84.00	95.00
Size um	60.56	34.33	12.56	3.472	0.890

R.Aire at Beale on 13.12.95

freshec.$07

File name:	FRESHEC.$07	Group ID:	FRESHEC
Sample ID:	Al.8	Run number:	2
Operator:	DMT		
Comments:	DISPERSED IN CALGON		
Start time:	10:47 9 Sep 1996	Run length:	60 Seconds
Pump Speed:	48		
Obscuration:	10%		
Optical model:	Fraunhofer		
LS 130	Fluid module		
Software:	1.50	Firmware:	1.3 1.8

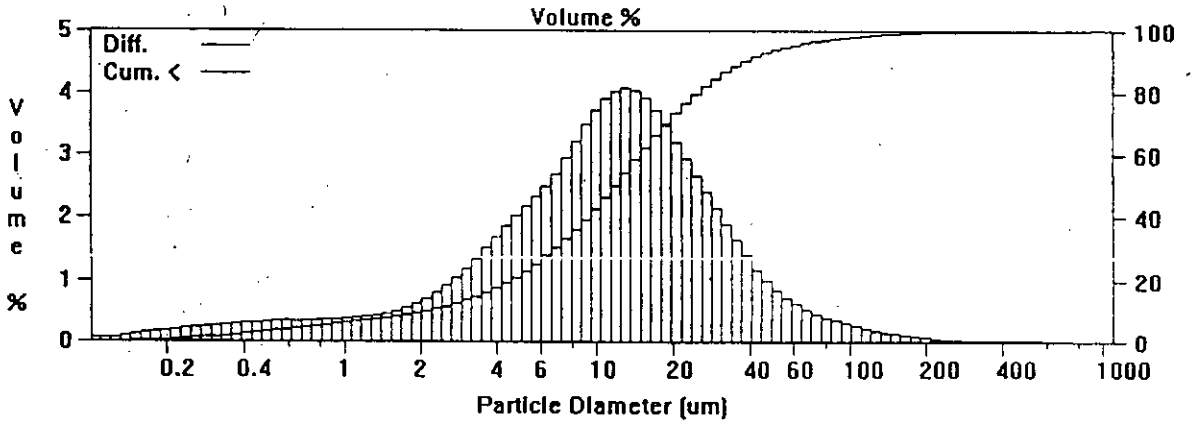

Volume Statistics (Arithmetic) freshec.$07

Calculations from 0.10 um to 900.00 um

Volume	100.0%		
Mean:	18.28 um	95% Conf. Limits:	12.41-24.14 um
Median:	11.33 um	Std. Dev.:	29.91 um
Mean/Median Ratio:	1.613	Variance:	894.7 um^2
Mode:	13.05 um	Coef. Var.:	163.7%
		Skewness:	8.049 Right skewed
		Kurtosis:	103.5 Leptokurtic

% >	5.000	16.00	50.00	84.00	95.00
Size um	54.74	27.55	11.33	3.441	0.714

R. Aire at Beale on 21.6.96

File name:	FRESHEC.$11	Group ID:	FRESHEC
Sample ID:	AI 0696.6	Run number:	6
Operator:	DMT		
Comments:	DISPERSED IN CALGON		
Start time:	12:06 9 Sep 1996	Run length:	61 Seconds
Pump Speed:	48		
Obscuration:	11%		
Optical model:	Fraunhofer		
LS 130	Fluid module		
Software:	1.50	Firmware:	1.3 1.8

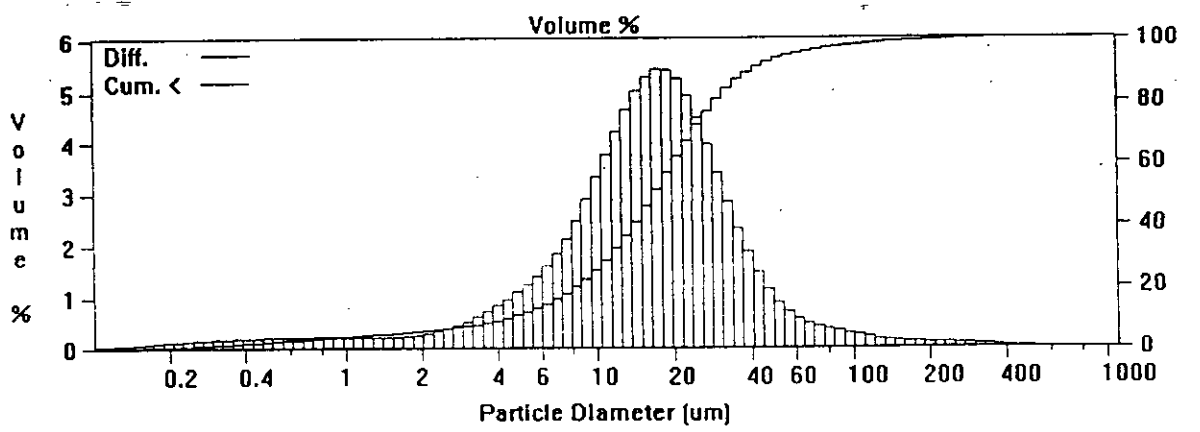

Volume Statistics (Arithmetic) freshec.$11

Calculations from 0.10 um to 900.00 um

Volume	100.0%		
Mean:	22.36 um	95% Conf. Limits:	16.00-28.71 um
Median:	16.01 um	Std. Dev.:	32.44 um
Mean/Median Ratio:	1.397	Variance:	1052 um^2
Mode:	17.15 um	Coef. Var.:	145.1%
		Skewness:	7.244 Right skewed
		Kurtosis:	73.53 Leptokurtic

%>	5.000	16.00	50.00	84.00	95.00
Size um	54.95	30.79	16.01	6.639	1.619

Appendix 2.

Interactions of Flutriafol with the surfaces of silica and layer silicates

Paper for submitted to Colloids and Surfaces (1996) for publication.

Abstract The mechanism of adsorption of flutriafol (CAS #76674-21-0), a large polyfunctional molecule used in fungicide formulation, from aqueous solution on the surface of kaolinite, montmorillonite, and silica gel has been studied combining the use of classical adsorption and kinetic experiments with modern computational methods of chemistry, such as AM1, PM3-MNDO, molecular mechanics, and molecular dynamics. Measurements are reported of the of the adsorption isotherms at 20 °C and diffusion kinetics of flutriafol in consolidated adsorbents. The contribution of different interactions to the total bonding energy has been compared. Hydration effects and hydrogen bonding dominate the adsorption from aqueous solutions; the characteristics of the most important hydrogen bonds and heats of hydration are reported. Possible influences on the adsorption isotherm of the acid-base reactions involving the adsorbate are discussed. The results suggest that flutriafol does not penetrate the interlayer spacing of K^+-montmorillonite in the conditions studied, but interacts only with the edge sites with an affinity similar to that measured for K^+-kaolinite.

Key words Adsorption mechanism, clay, hydrogen bonding, flutriafol, silica gel, kaolinite, montmorillonite, AM1, PM3.

INTRODUCTION

The mechanism of sorption of organic molecules by silica and layer silicates is not yet fully understood, mainly because the factors controlling the interactions vary from system to system. It is usually supposed that the bonding of microorganic compounds occurs by one of the following mechanisms:

(i) replacement of exchangable inorganic cations by organic cations;
(ii) hydrogen bonding of the type NH...O, OH...O, CH...O, etc.;
(iii) van der Waals attraction, which can dominate adsorption of large molecules and ions;
(iv) electrostatic interaction;
(v) coordination to interlayer cations.

Comprehensive reviews of the subject are available [1,2].

Most studies of the interaction mechanism utilize infrared spectroscopy [3-6] to probe changes in the adsorbate environment. However, the applicability of this technique is limited to reactions on dry surfaces or use in non-aqueous solution, whereas many effects of practical importance are related to the solid/aqueous solution interface.

The 8th edition of *The Pesticide Manual* [7] lists more than one thousand formulations of commercial pesticides, and considering the number of known minerals, it does not seem practicable to investigate all possible adsorbate/adsorbent combinations. However the underlying physicochemical principles governing adsorption are common to many of these systems and are worthy of investigation.

This study, combining classical adsorption and kinetic experiments and modern chemical computational methods, examines the adsorption of a relatively complex pesticide molecule, (RS)-2,4′-difluoro-α-(1H-1,2,4-triazol-1-ylmethyl)-benzhydryl alcohol, more often known under the trivial name, flutriafol [7], on the surface of kaolinite, montmorillonite and silica gel.

EXPERIMENTAL

Preparation of Aqueous Solutions of Flutriafol. The desired initial concentration of flutriafol in the solutions used in the kinetics and adsorption experiments was prepared by diluting the 1.0 mg dm^{-3} aqueous stock solution of the pesticide. To prepare the latter, 8 ml of 200 mg dm^{-3} stock solution, which

had in turn been prepared by dissolution of a weighted amount of flutriafol (*Analytical Standard, IOIC*) in ethylacetate (*Fisher*), were placed in 1000 ml volumetric flack and ethylacetate was evaporated by the flow of dry nitrogen. The residue was dissolved in 1000 ml of 0.01M aqueous solution of potassium hydrogen carbonate (AR grade, *BDH*) by stirring overnight and the solution filtered through a 0.45 μm cellulose nitrate membrane.

Determination of the Concentration of Flutriafol. To determine the concentration of flutriafol in a solution, the pesticide was extracted on a C_{18} chromatographic column (*Bakerbond SPE, IST*), eluted by ethylacetate, the eluate dried with Na_2SO_4 (granular, AR grade, cured at 160 °C) and analysed with an automated GC/MS instrument (*Hewlett Packard G1034C MS ChemStation*) equipped with a *Hewlett Packard 5890 Series II Gas Chromatograph.* The sample was introduced via a split/splitless injector to a 5% phenyl methylpolysiloxane capillary column (25 m, 0.2 mm, 0.33 μm film thickness) with He as the carrier gas. The oven program was 15 °C min^{-1} to 170 °C, 5 °C min^{-1} to 240 °C, 2 °C min^{-1} to 270 °C and held at this temperature for 10 min. The analysis was based on detection of peaks of a target ion (*m/z* 123) and a qualifier ion (*m/z* 164), the retention time being 22.3 min. The instrument was recalibrated before each measurement using at least three standard solutions with decachlorobiphenyl internal standard (*m/z* 178 and 240). In order to avoid any errors caused by possible hydrolysis or photolysis of flutriafol, its concentration in the aqueous stock solution was redetermined each time it was used.

Pretreatment of Adsorbents. Kaolinite and montmorillonite were first treated with 30% hydrogen peroxide to remove traces of organic substances, then washed several times with distilled water, and transformed to the K^+-form by treatment with 1M solution of potassium chloride as described elsewhere [8]. After final washing, the clay was dried at 120 °C and powdered in a mortar. Silica gel (surface area 300 $m^2 g^{-1}$, pore volume 1.6 $cm^3 g^{-1}$; Johnson Matthey GmbH) was used as received.

The specific surface area of kaolinite was 9.5 $m^2 g^{-1}$ by multipoint BET analysis. The total surface area of delamellarized montmorillonite was 462 $m^2 g^{-1}$ by the adsorption of water.

The mineral percentage of the clays determined by X-ray difraction was as follows: kaolinite samples (kaolinite 92.2%, illite/mica 4.3%, and quartz 3.5%);

montmorillonite samples (montmorillonite 66.5%, quartz 13.8%, feldspar 17.8%, and sylvite 1.8%).

Adsorption Experiment. Weighed amounts of adsorbent were placed in glass bottles containing known amounts of flutriafol in 0.01M aqueous $KHCO_3$ solution. The initial pH of the solutions was adjusted to pH 7 by bubbling a CO_2/N_2 gas mixture. The bottles were immediately closed and shaken overnight at 20 °C. Separation of sediments from the dispersion was performed either by filtration on a 0.45 μm filter (kaolinite and silica gel) or by centrifugation at 6000 r.p.m. (montmorillonite). The concentration of flutriafol in the initial solution and in the filtrate was determined as described before. The experimental technique and precautions necessary in adsorption measurements are discussed more fully elsewhere [8-10].

Kinetic experiment. Adsorption to a packed bed of adsorbent was measured at room temperature using a pyrex glass apparatus consisting of a 200 ml reservoir of aqueous flutriafol (initial concentration 0.2 μmol dm^{-3}) mounted on the top of a 4 cm cylindrical pot containing adsorbent. The adsorbent was separated from the overlying solution by a 1 mm metal grid to minimize any disturbance of the adsorbent phase. The change in the concentration of flutriafol was measured over a period of one month by sampling 10 mls at intervals. The apparent porosity of sorbents was estimated using the water pycnometry [11].

ADSORPTION ISOTHERMS AND ADSORPTION KINETICS

In the concentration range studied, adsorption of flutriafol on all three adsorbents follows the Henry law (Fig. 1). Adsorption equilibrium was established in less than 1 hour when the adsorbent was in suspension, and so, the adsorbent/solution contact area was at a maximum. When the adsorption rate is limited by diffusion, the equilibrium time increases by many orders of magnitude.

Often with natural minerals the specific surface area is difficult to determine or is uncertain because of the changes in particulate structure which occurs during drying. In such situations, the adsorption is conventionally expressed by a distribution coefficient, K_d, defined as the ratio of the weight concentration of adsorbate on the surface to its equilibrium concentration in the solution, so that $K_d = \Gamma S_{sp} \cdot 10^6$ dm^3 g^{-1}, where S_{sp} is the specific surface area. So

determined, K_d's for kaolinite, montmorillonite and silica gel are 1.6, 39.7 and 8.7 $dm^3\,kg^{-1}$, respectively, and well in the range found for natural sediments.

When flutriafol is adsorbed by a sufficiently thick undisturbed layer of adsorbent, the adsorption kinetics are described by a one-dimensional semi-infinite diffusion model with adsorbate binding [12,13]. In summary: let the adsorption equilibrium become settled at each point of the adsorbent phase for a so short time that the overall concentration profile remains almost unaltered. The adsorption, $a(x,t)$, which here is measured in moles per unit volume of the adsorbent phase, in the point x at the time t is then related to the concentration, $c(x,t)$, of adsorbate in the neighbourhood of this point by a local isotherm equation, the simplest of which is due to Henry,

$$a(x,t) = \iota S_{sp} \Gamma c(x,t) \qquad (1)$$

where ι is the pycnometric density, and Γ is the Henry constant.

Except for the case of strong localized adsorption, both the dissolved and adsorbed molecules can be involved in the diffusion motion. Let D_s and D_a be the corresponding diffusion coefficients. The governing equations are

$$\lambda \frac{\partial c}{\partial t} = D_s \frac{\partial^2 c}{\partial x^2}; \quad (1-\lambda)\frac{\partial a}{\partial t} = D_a \frac{\partial^2 a}{\partial x^2} \qquad (2)$$

where λ is the porosity. After substitution of eqn.(1) for a and adding the above two equations, one gets

$$\frac{\partial c}{\partial t} = \delta^2 \frac{\partial^2 c}{\partial x^2}; \quad \delta^2 = \frac{D'}{\lambda + \Gamma'(1-\lambda)}; \quad \Gamma' = \iota S_{sp}\Gamma; \quad D' = D_s + \Gamma' D_a \qquad (3)$$

where D' is termed the effective diffusion coefficient.

Finally, imposition of the boundary conditions,

$$c(0,t) = c(t); \quad c(x,0) = 0, \qquad (4)$$

$c(t)$ being the concentration of the adsorbate in the outer solution, and the mass balance requirement,

$$\{\lambda + \Gamma'(1-\lambda)\}\int_0^\infty c(x,t)\mathrm{d}x = L\{c(0) - c(t)\}, \qquad (5)$$

where L is the effective depth of the overlying solution, and the upper bound of integration has been extended to infinity in view of the assumtion that $x >> (D't)^{1/2}$, leads to

$$c(t) = c(0)\exp(\pi A^2 t)\mathrm{erfc}(A\sqrt{\pi t});\ A^2 = \frac{D'(\lambda + \Gamma'(1-\lambda))}{\pi L^2} \qquad (6)$$

As $t \to 0$, this reduces to

$$c(t) \cong c(0)\left[1 - 2At^{1/2}\right] \qquad (7)$$

Proportionality of the concentration to the square root of time is a characteristic of diffusion-controlled processes [14,15]. Eqs.(6) and (7) were obtained in an earlier work [13], but the coefficient A was unfortunately determined incorrectly.

The corresponding kinetic curves for flutriafol adsorption on the sorbents under study are represented in Fig. 2. It should be noted that the diffusion coefficient of flutriafol proves to be of the same order of magnitude as the coefficients of self-diffusion of alkylammonium ions in wet montmorillonite [16].

THE MECHANISM OF BONDING

Chemical Interactions

Description of Molecular Models.

The surface of colloidal particles of montmorillonite and kaolinite was simulated using clusters composed of one to three disc-shaped fragments having the formulas $Si_{102}O_{318}Al_{57}H_{83}$ (M = 9574.1) and $Si_{54}O_{235}Al_{57}H_{109}$ (M = 6924.3), respectively, and radius of approximately 14 A. An example of such a model is shown in Fig. 3. Taking into account the globular structure of silica gel [17], its surface was simulated by a spherical cluster $Si_{51}O_{131}H_{58}$ (M = 3586.7) having radius of approximately 8.5 A and lattice of β-crystoballite. All the clusters were constructed on the basis of the crystallographic data [18] and optimised using the extended MM2 force field [19]. To avoid the undesirable distortion of the kaolinite and montmorillonite clusters during optimisation, all the octahedral positions were filled with Al atoms. The resulting trioctahedral structures inevitably possess an excess positive charge, whereas the naturally occurring dioctahedral structures are known to be negatively charged [20,21]. To overcome this difficulty, all the Al atoms were assigned an effective charge lower than the charge of Al^{3+} ions. This can be imagined as uniform isomorphous substitution of a part of the Al^{3+} by Mg^{2+} ions as occurs in nature.

For semiempirical calculations, clusters of smaller size, containing the functionality of interest, were isolated from the large clusters and the broken bonds saturated with pseudoatoms [22].

Information concerning the hydration energy, sorption capacity, and other similar characteristics of the surface may be obtained by counting the different functional groups at the cluster surface and assessment of the cluster size. Thus, on the basis of the described models, the density of siloxane bridges, SiOSi, at the basal plane of layer silicates is estimated to be 15.5 nm^{-2}, whereas the density of the bridge hydroxyl groups coordinated to Al ions is only 3.2 nm^{-2}. The density of surface silanols, SiOH, at the edge surface is found to be 3.8 nm^{-2}. It is also evident that the ratio of the amount of groups situated at the basal plane to the amount situated at the edge is proportional to the radius of the cluster.

The density of surface silanols at the completely hydroxylated surface of silica is estimated as 6.4 nm^{-2}, almost six times the value commonly accepted for the density of *isolated* silanols at the surface of *dry* silica gel [23-25]. A possible explanation is that the geminal silanol groups representing the majority at the surface of the model cluster, are unstable and easily eliminate water while drying.

Theoretical Assessment of the Hydration Energy of the Surface

To calculate the hydration energy of a mineral surface, it is necessary to estimate (i) the energy of association of water molecules with different polar groups resident at the surface and (ii) the density of these groups. The latter has just been done in the previous section. The energy of association, in this context termed usually as hydrogen bonding, in the structures shown in Fig. 4-a has been calculated using the semiempirical methods AM1 [26-29] and PM3-MNDO [30]. Fig. 4-b shows the cluster $Si_{12}O_{34}Al_4H_{14}$ used in the calculation. The use of pseudoatoms was made whenever it seemed to be justified. The choice of the structures to be considered is not unique and has been made on the basis of chemical intuition. The possibility of the direct coordination of water molecules to silicon atoms was examined elsewhere [24] and is not discussed here. The characteristics of the calculated H-bonds are summarised in Table 1.

It is rather unexpected that the most acidic bridged hydroxyl groups fail to bond water. A possible explanation is as follows: In order for a water molecule to satisfy the geometrical criteria enabling hydrogen bonding, it has to be orientated over the SiOSi plane, leading to strong repulsion between the non-bonding electron pairs of the oxygen atoms (Fig. 4-c). This causes the water molecule to realign, so that it forms a hydrogen bond of the type 2 instead.

Both hydrogen bonding and orientation of water molecules in the potential field of the surface contribute to the hydration energy. However, once the use of the above-mentioned parametrical methods is made, there is little point in trying to assess the role of the orientation effect separately (although it is possible on the basis of existing macroscopic theories [31]), since these methods have been parametrized to describe, with the best possible precision, a large number of molecular properties including intermolecular interactions. However, if these methods predict attraction between two molecules, it is not always possible to say definitely whether this is a hydrogen bond or just the dispersion interaction. This is why some additional geometrical criteria concerning the bond length and angle are used [32,33]. Nevertheless, without exact stipulation of the meaning of "hydrogen bond", the hydration energy of a surface can be estimated by summing the calculated heats of formation of the hydrogen bonds between water and polar groups situated at that surface. This yields 0.088 - 0.098 cal m^{-2} of the basal plane, and 0.015 - 0.041 cal m^{-2} of the edge surface.

An independent estimate of the hydration energy has been gained from a molecular dynamic simulation of a periodic box with a cluster of interest surrounded by up to 500 water molecules (MM2 force field, HyperChem software). This gives approximately 0.015 kcal m^{-2} for T = 298 K, and, as expected taking into view the underlying approximations of the method, the result is almost independent of the chemical speciation of the surface. Multiplying this result by the surface area of the clusters and dividing by their molecular mass yields an estimate of 26 - 38 cal g^{-1} of dry substance. The available literature data on heats of immersion vary in the range 16 - 35 cal g^{-1} [34-36], and are in essential agreement with the theoretical predictions.

Theoretical Assessment of the Hydration Energy of Flutriafol

Following the above considerations, the energies of the most realistic hydrogen bonds arising between water and the polar functional groups of flutriafol have been calculated. The results are summarised in Table 2. The following sketch explains the bond notation used in this paper.

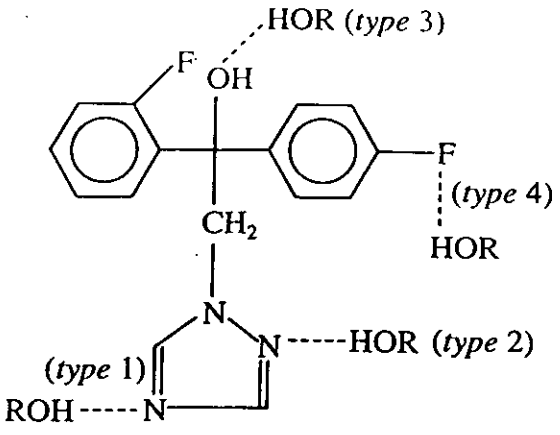

R = H; $Si(OH)_3$; $Si_{10}O_{27}H_{15}$; $Si_{12}O_{33}Al_4H_{13}$

There also exists the probability of weak hydrogen bonds ($-\Delta H_f \cong 1.0$ kcal mol^{-1}) with the methylene group. The characteristics of the hydrogen bonds with the fluorine atoms in *ortho* and *para* positions are nearly identical. The total hydration energy of flutriafol is thus estimated to be 22.6 kcal mol^{-1} by AM1 and 13.8 kcal mol^{-1} by PM3-MNDO. Molecular dynamics simulation (MM2 force field) of a periodic box containing 244 water molecules surrounding a flutriafol molecule yields 21.6 kcal mol^{-1} at 298 °K.

It is commonly assumed that the protonated or cationic form of most pesticide molecules should be considered as weakly hydrated. This belief most likely stems from a misinterpretation of the fact that the hydration of cations weakens with their increasing size, as occurs, for example, in the series $Li^+ > K^+ > NMe_3^+ > NBu_3^+$. Most pesticide molecules, including flutriafol, are polyfunctional, and deactivation of a given functional group by protonation does not preclude hydration of the whole molecule if there are other functional groups capable of bonding with water.

Interaction of Flutriafol with the Surface

Flutriafol can form stable hydrogen bonds with the surface of montmorillonite, kaolinite, and silica. With the silica gel surface and the edge surface of kaolinite and montmorillonite, hydrogen bonding is primarily effected through the free silanol groups [37-40]. The characteristics of the most probable bonds of this type are given in Table 3. The bond notation is the same as before. For comparison, heats of adsorption of alcohol on silica glasses fall into the range of 5.7 to 10.0 kcal mol^{-1} [41].

The only stable hydrogen bond with the basal plane is through the alcohol hydroxyl group of flutriafol to a bridge siloxane oxygen. Its characteristics are as follows: (AM1) $-\Delta H_f$ = 2.9 kcal mol^{-1}, d(H...O) = 2.73 A, $\angle$(O-H...O) = 169.0°; (PM3-MNDO) $-\Delta H_f$ = 0.2 kcal mol^{-1}, d(H...O) = 1.87 A, $\angle$(O-H...O) = 168.0°. The relatively low energy of this bond conforms to the fact that the siloxane oxygen is a weak donor of electrons [24,38].

Hydrogen bonding through the bridge hydroxyl groups situated at the apices of AlO_6 octahedra is sterically hindered by a crown of six SiO_4 tetrahedra making these groups inaccessible to large molecules. If this crown is removed by displacement of the SiO_4 tetrahedra by hydrogen atoms, the hydrogen bonding is enabled. Such displacement may occur in the vicinity of the lattice edge due to preferential dissolution. An example of such a hydrogen bond is shown in Fig. 5. Its high energy arises because of participation of the π-electron aromatic system of the triazole group in the bonding, so that the formed adduct has some properties of a π-complex. To this end, because of high acidity of the bridge hydroxyl groups [42], complete transfer of proton to flutriafol seems more probable.

In the case of montmorillonite, an expandable clay, there is also the possibility for fixation of flutriafol by coordination to the interlayer exchangable cations [43-45], as, for example, shown in Fig. 3. Such coordination can be through any electron-donating groups, such as triazole, hydroxyl, and to a smaller extent, fluorine and aromatic rings. Bonding through the triazole group is the strongest, with the bond energy for univalent cations calculated by AM1 and PM3-MNDO as 9.8 - 9.9 kcal mol^{-1}, rising to 27.4 - 29.1 kcal mol^{-1} for divalent cations. When coordinated to certain transition metal ions, the bonding is expected to be even stronger because of the presence of *d*-orbitals. However, as shown by comparison of the adsorption to montmorillonite and kaolinite, no appreciable adsorption to the interlayer of montmorillonite occurs. One reason for this behaviour is as follows. In the case of small and therefore strongly hydrated cations, such as Li^+ and Mg^{2+}, where the interlayer spacing is large enough to allow accommodation of a flutriafol molecule, water is a better candidate for a place in the coordination sphere and displaces flutriafol. Coordination of water also reduces the polarising power the ions. In contract, for large cations, such as

K^+ and Ba^{2+}, with weaker hydration, there is nothing to prevent flutriafol from the coordinating, however the interlayer spacing is reduced leaving insufficient room for a bulky flutriafol molecule to penetrate. This means that flutriafol is mainly adsorbed at the edge surface and explains why the observed adsorption of flutriafol on K^+-montmorillonite is similar to K^+-kaolinite. Another reason for the discrepancy is that the penetration of a flutriafol molecule to the interlayer space inevitably results in displacement of several water molecules from the relatively highly ordered hydration shell of the surface, thereby increasing the free energy of the system.

It is of interest to examine, at least at a qualitative level, how the probability of entrance of flutriafol to the interlayer space depends onto the interlayer separation. A system similar to that shown in Fig. 3 has been modelled. A flutriafol molecule was placed in the plane lying between the two halves of a two-disc montmorillonite cluster parallel to their basal surface at a distance of approximately 20 A from the edge. Then it was given an initial impetus to cause its movement toward the cluster. Its further trajectory was calculated according to the principles of molecular dynamics (HyperChem Software). The cluster was fixed, thus no dissipation of energy was allowed. Fig. 6 represents the result of molecular dynamic simulation of this process. It has been found that the activation energy increases rapidly as the interlayer separation becomes less than 12.6 A. On the contrary, if it is greater than approximately 16 A, the process can carry out without activation.

Protolytic Transformations and Adsorption

Bearing a base triazole functionality, flutriafol is involved in the acid-base reaction

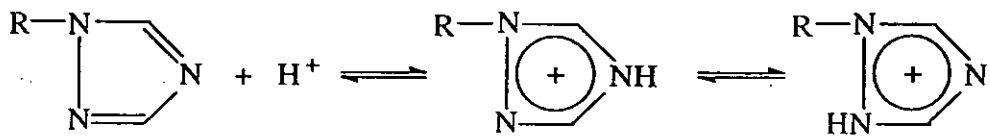

(I) (II)

with the conjugated acid existing in two tautomeric forms. The results of AM1 and PM3-MNDO calculation show that the cation I should be more stable than the cation II; the corresponding difference in the energy of formation is 7.9 - 12.7 kcal mol^{-1} in favour of the first ion. The polarizability of flutriafol (22.0 - 23.3 A^3)

is almost unaffected by protonation, whereas the dipole moment increases from 3.7 Debye for the deprotonated molecule to 9.7 - 13.3 Debye for the cation I, and to 8.3 - 8.9 Debye for the cation II. Both cations can form stable hydrogen bonds with water and surface silanols, and owing to their high dipole momenta and polarizabilities, undergo strong electrostatic attraction to the surface.

The relative affinity of the neutral and cationic forms of the adsorbate can affect the adsorption isotherm [46-48]. The adsorption of flutriafol is governed by the following system of stoichiometric equations,

$$\begin{aligned} \mathrm{Fl} + \mathrm{H^+} &\xleftrightarrow{K_p} \mathrm{FlH^+} \\ \mathrm{S} + \mathrm{Fl} &\xleftrightarrow{K_1} \mathrm{SFl} \\ \mathrm{S} + \mathrm{FlH^+} &\xleftrightarrow{K_2} \mathrm{SFlH^+} \end{aligned} \qquad (8)$$

each reaction being characterised by its equilibrium constant. Here Fl and FlH^+ designate the deprotonated and the protonated form of flutriafol, respectively, and S an adsorption site. The above equations describe what is generally called localised adsorption. However, without exact stipulation of the term "adsorption site", they remain valid for non-localised adsorption too. Under the conditions which Henry's law applies, i.e. [S] >> [SFl] + [$SFlH^+$], the amount of free adsorption sites is unaltered during adsorption. The system (8) can then be closed by adding a single mass balance equation,

$$V[\mathrm{Fl}]\left(1 + K_p[\mathrm{H^+}]\right) + mS_{sp}c_s[\mathrm{Fl}]\left(K_1 + K_2K_p[\mathrm{H^+}]\right) = c_{\mathrm{Fl}}^0 V \qquad (9)$$

where V is the volume of the solution, m and S_{sp} are the weight and the specific surface area of the adsorbent, c_s is the density of the adsorption sites (mol m^{-2}), and c_{Fl}^0 is the initial concentration of flutriafol in the solution. Now, the amount of flutriafol adsorbed per unit surface is given by

$$n_{\mathrm{Fl}}^{\mathrm{ads}} = \frac{c_s c_{\mathrm{Fl}}^0 V\left(K_1 + K_2K_p[\mathrm{H^+}]\right)}{V\left(1 + K_p[\mathrm{H^+}]\right) + mS_{sp}c_s\left(K_1 + K_2K_p[\mathrm{H^+}]\right)} \qquad (10)$$

If only the cationic form of flutriafol is capable of adsorption, eqn.(10) can be simplified by putting $K_1 = 0$. The adsorption then becomes independent of pH when $K_p[H^+] >> 1$. If only the neutral form is capable of adsorption, the adsorption becomes independent of pH when $K_p[H^+] << 1$. Finally, if the protonated and deprotonated forms have similar adsorption affinities, i.e. $K_1 \cong K_2 \cong K$, the adsorption is always independent of pH,

$$n_{Fl}^{ads} = \frac{c_s c_{Fl}^0 VK}{V + mS_{sp} c_s K} = \Gamma c_{Fl}^0 \qquad (11)$$

where Γ is the Henry's law constant.

The protonation constant, K_p, of the triazole group of flutriafol is not likely to differ much from that of imidazole ($pK = 6.95$). Therefore, the protonated and deprotonated forms coexist at similar concentrations at pH close to 7. Nevertheless, the adsorbed state flutriafol is expected to be entirely protonated, irrespectively of which form predominates in the solution. This hypothesis is based on the fact that the surface of silica and clays possess a negative charge in the pH range of interest [12]. Let $-\psi_s$ be its electrostatic potential, which attains a value of 80 - 100 mV at pH ≅ 7. Then, in accordance with the generalised mass action law [11], the effective protonation constant of adsorbed molecules increases by a factor of $\exp(e\psi_s / kT)$ relative to the protonation constant, K_p, characteristic of molecules in the bulk solution. Hence, with high acidity of surface silanols and bridge hydroxyl groups, protonation of adsorbed flutriafol is highly probable.

The possibility of protonation of a given compound depends upon its pK, and also upon pH of the surrounding solution. Thus, many amines and amides are known to be protonated when adsorbed onto clays [49-51], whereas atrazine not [52]. However, the possibility of protonation of some very basic amines, such as propylamine and ethylendiamine, has been questioned by the authors of paper [53].

Physical Interactions

A study of the physical interactions of flutriafol to a mineral surface has been performed on the basis of a computer simulation of interactions between a flutriafol molecule and a montmorillonite cluster composed of two disc-shaped fragments $Si_{102}O_{318}Al_{57}H_{83}$ with the interlayer spacing of 12.6 A. A similar system is shown in Fig. 3. The potential energy function used was as follows

$$U = \sum_i \sum_j \varsigma\left[(\kappa / R_{ij})^{12} - 2(\kappa / R_{ij})^6\right] - \mathbf{p} \cdot \mathbf{E} - \frac{1}{2}(\alpha \mathbf{E}) \cdot \mathbf{E} \qquad (12)$$

where the first term represents the well-known Lennard-Jones 6-12 potential to allow for the van der Waals interactions between atoms. The last two terms describe, in a highly approximative manner, the long-range electrostatic interactions, such as the interaction of the permanent dipole, p, and the induced

dipole, αE, of the adsorbate molecule, which is considered as a rigid anisotropic spheroid with a polarizability tensor α, with the electric field, E, produced by the cluster. An important role of the electrostatic interaction in adsorption on polar surfaces has also been emphasised in papers [54,55]. In eqn.(12), R_{ij} is the distance between the ith atom of the cluster and the jth atom of the molecule, and ζ and κ are, correspondingly, the intensity and the width parameters characterising the shape of the atom-atom potential [56]. For the sake of simplicity, the latter have been taken the same for all atoms. A constant term corresponding to the interactions within the groups of atoms belonging separately to the cluster and the flutriafol molecule has been omitted since it does not affect the further results.

It is convenient to use the principal axes of inertia of the cluster and of the adsorbate molecule as the axes of the local coordinate systems bound to the cluster and to the molecule, respectively. Then

$$\mathbf{E}(\mathbf{R}) = \sum \frac{\rho_i e(\mathbf{R}-\mathbf{r}_i)}{\varepsilon|\mathbf{R}-\mathbf{r}_i|^3}; \quad R_{ij} = |\mathbf{R}-\mathbf{r}_i+\mathbf{r}_j'| \qquad (13)$$

where ρ_i is the charge number of the ith ion of the cluster, ε is the dielectric constant of the medium, $\mathbf{r}_i$ is the position of the ith ion of the cluster and $\mathbf{r}_j'$ is the position of the jth ion of the molecule in their local coordinate systems, and R joins the origin of the first coordinate system to the origin of the second. It is not yet clear how to determine the distance between the cluster and the molecule, unless they are point-wise. If it is intended to analyse the interaction with the basal plane and the edge surface only, it is convenient to direct the z-axis of the first coordinate system towards the adsorbate molecule and to place the latter so that its centre of gravity is on this axis. Then the separation, s, between the basal plane and the molecule can be determined as

$$s = |\mathbf{R}| - \max_i\left(\frac{\mathbf{r}_i\cdot\mathbf{R}}{|\mathbf{R}|}\right) - \min_j\left(\frac{\mathbf{r}_j'\cdot\mathbf{R}}{|\mathbf{R}|}\right), \quad \mathbf{E}(s) \cong \frac{(\mathbf{E}\cdot\mathbf{R})}{\mathbf{R}^2}\mathbf{R}, \text{ and } |\mathbf{R}| \cong z \qquad (14)$$

In view of the made assumptions, U is also dependent on the three Euler angles, η, θ, and ϕ, necessary to define the orientation of the adsorbate molecule with respect to the cluster. Hence, U must be averaged over these angles with the Boltzmann weighting factor to allow for the contribution of different orientations [56],

$$\overline{U} = N\int U \exp(-U / kT)\mathrm{d}\eta\mathrm{d}\theta\mathrm{d}\phi \qquad (15)$$

N being the normalising factor.

The integration in eqn.(15) was performed numerically, leading to the results shown in Fig. 7. The parameters used in the computations are given in Table 4. The dipole moment and polarizability of the ground state of a flutriafol molecule have been calculated using the AM1 method [25,27]. The effective charges on the atoms of Si, O, and H have been taken the same as those calculated for the cluster $Si_{10}O_{28}H_{16}$ [57]. The effective charge of the Al atoms has been assigned to ensure electroneutrality of the whole cluster. The dielectric constant, ε, has arbitrarily been assigned a value of 10, to account for a reduction in the dielectric constant of water close to the surface.

As indicated in Fig. 7, the interaction of flutriafol with the flat basal surface is much stronger that with the rough edge surface. As shown previously, specific interactions, such as hydrogen bonding, may change the entire energy balance. In the absence of the latter, the Henry constant is determined by the relation [58]

$$\Gamma = \int_0^\infty \left[\exp(-\overline{U} / kT) - 1\right]\mathrm{d}s \qquad (16)$$

and is equal to $2.6 \cdot 10^{12}$ m for the basal plane, and only $3.9 \cdot 10^{-5}$ m, seventeen (!) orders of magnitude less, for the edge. The latter value depends considerably upon the cluster size and the interlayer spacing, and can be much higher for a concave surface. Consequently, if physical interactions dominated adsorption, a very strong dependence of the Henry constant on the dispersity of adsorbent would be expected. Although such a dependence does take place, it is minimal, suggesting that the role of the physical interactions is relatively small, at least for the adsorption from aqueous solutions, in comparison with the role of the chemical interactions discussed before.

The experimentally determined value of the Henry constant can be related to the quantities introduced in the previous sections in the following way. Writing

$$\Gamma = \gamma \exp(-\Delta H / kT) \qquad (17)$$

where γ depends only on the entropy change during adsorption. The total heat of adsorption, ΔH, is in a very crude approximation given by

$$\Delta H = \Delta H^a_{bond} + \overline{U}^a - n(\Delta H^s_{bond} + \overline{U}^s) \qquad (18)$$

where the superscripts a and s refer to the adsorbate and solvent, respectively, and n is the mean number of solvent molecules replaced by one adsorbate molecule during adsorption. Each molecule is assumed to be bonded with the surface, the heat of bonding being ΔH_{bond}, and is subject to the action of the potential field of the surface. An additional term must be added to eqn. (18) if the adsorbate is known to lose a part of its hydration shell while being adsorbed.

The number of the solvent molecules being replaced during adsorption can be estimated as the ratio of molecular volumes of adsorbate and solvent; for the flutriafol/water pair $n \equiv 22$. In a hypothetical case of the absence of solvent (a gas-phase process) $n = 0$, so the Henry constant can be expected to be very high. To some extent, this should hold for adsorption from non-polar solvents, in which case ΔH^s_{bond} and $\overline{U}^s$ are relatively small. On the contrary, for the adsorption from aqueous solutions, the bonding energy of water, ΔH^s_{bond}, is close to that of flutriafol, ΔH^a_{bond}, leading to the low values of the Henry constant observed.

CONCLUSION

The adsorption of flutriafol from aqueous solution at 20 °C on kaolinite, montmorillonite and silica gel follows the Henry law for equilibrium concentrations of the order of 1 μmol dm^{-3} with the adsorption affinity changing in the sequence: kaolinite > montmorillonite > silica gel. The lower affinity of flutriafol to montmorillonite compared with kaolinite suggests that flutriafol does not enter the interlayer space of the clay but bonds to the edge sites. Estimates of the physical interaction energy indicate that the degree of dispersity of clay should have a very strong effect on the adsorption. However, this is not observed experimentally, suggesting physical interactions are not dominant for the systems in question. Molecular calculations indicate a weak interaction dominated by the hydration and hydrogen bonding effects. It is also possible that the triazole base interacts with the acidic bridged hydroxyl groups by the acid-base mechanism.

The results of adsorption and kinetic measurements have been applied to estimate the effective diffusion coefficients of flutriafol in consolidate adsorbents using the model of semi-infinite diffusion with adsorbate binding. The obtained diffusion coefficients are of magnitude typical of molecular diffusion in gels.

REFERENCES

[1] J.A. Raussell-Colom and J.M. Serratosa, in A.C.D. Newman (Ed.), Chemistry of Clays and Clay Minerals, Mineralogical Society, Avon, 1987, chap. 8, p. 371.

[2] W.A. House, in N. Claver (Ed.), Environmental Interactions of Clay Minerals, Springer-Verlag, Berlin, 1997 (in press).

[3] J.D. Raussell, Trans. Faraday Soc., 61 (1965) 2284.

[4] V.C. Farmer and M.M. Mortland, J. Phys. Chem., 69 (1965) 683.

[5] V.C. Farmer and J.D. Russell, Clays Clay Minerals, 15 (1966) 121.

[6] J.L. White, Proc. Int. Clay Conf., Wilmette, Illinois, 1975, p. 391.

[7] C.R. Worthing (Ed.), The Pesticide Manual. A World Compendium. 8th ed., BCPC, Lavenham, Suffolk, 1987.

[8] W.A. House and I.S. Farr, Colloids Surf., 40 (1989) 167.

[9] J.L. Huang and C.S. Liao, J. San. Eng. Division, 5 (1970) 1057.

[10] W.A. House and Z. Ou, Chemosphere, 24 (1992) 819.

[11] D.G. Jeffs, W.B. Jepson and J.B. Rowse, J. Colloid Interface Sci., 49 (1974) 256.

[12] B.V. Zhmud and A.A. Golub, Colloids Surf. A., 105 (1995) 173.

[13] B.V. Zhmud, A.B. Pechenyi and V.A. Kalibabchuk, Ukr. Khim. Zh., 61 (1995) 11.

[14] J. Crank, Infinite and Semi-Infinite Media, Oxford University Press, London, 1975.

[15] D.A. Frank-Kamenetskii, Diffusion and Heat Transfer in Chemical Kinetics, Nauka, Moscow, 1967.

[16] R.G. Gast and M.M. Mortland, J. Colloid Interface Sci., 37 (1971) 80.

[17] A.V. Kiselev, Kolloidn. Zh., 2 (1936) 17.

[18] R.E. Grim, Clay Mineralogy, McGraw-Hill, New York, 1968.

[19] K.B. Lipkowitz, QCPE Bulletin, 12 (1992) 6.

[20] S. Yariv and H. Cross, Geochemistry of Colloid Systems, Springer-Verlag, Berlin, 1979.

[21] K.A. Wierer and B. Dobias, J. Colloid Interface Sci., 122 (1988) 171.

[22] H.H. Dunken and V.I. Lygin, Quantenchemie der Adsorption an Festkorperoberflachen, VEB Deutscher Verlag fur Grundstoffindustrie, Leipzig, 1978.

[23] L.T. Zhuravlev, Langmuir, 3 (1987) 316.

[24] A.A. Chuiko and Yu.I. Gorlov, The Surface Chemistry of Silica, Naukova Dumka, Kiev, 1992.

[25] V.Ya. Davydov, A.V. Kiselev, S.A. Kiselev, et.al., J. Colloid Interface Sci., 74 (1980) 378.

[26] M.J.S. Dewar, E.G. Zoebish, E.F. Healy and J.J.P. Stewart, J. Am. Chem. Soc., 107 (1985) 3902.

[27] M.J.S. Dewar and C. Jie, Organomet., 6 (1987) 1486.

[28] M.J.S. Dewar and E.G. Zoebish, J. Mol. Struct. (Theochem), 180 (1988) 1.

[29] M.J.S. Dewar and A.J. Holder, Organomet., 9 (1990) 508.

[30] J.J.P. Stewart, J. Comp. Chem., 10 (1989) 209.

[31] S. Kirchner and G. Cevc, J. Chem. Soc., Faraday Trans., 90 (1994) 1941.

[32] S. Vinogradov, in H. Ratajczak and W.J. Orville-Thomas (Eds.), Molecular Interactions, Wiley, New York, 1981.

[33] N.D. Sokolov, in N.D. Sokolov (Ed.), The Hydrogen Bond, Nauka, Moscow, 1981, p. 63.

[34] R. Greene-Kelly, Clay Miner. Bull., 5 (1962) 1.

[35] D.M. Anderson and G. Sposito, Soil Sci., 97 (1964) 214.

[36] R. Keren and I. Stainberg, Clays Clay Miner., 23 (1975) 193.

[37] P.A. Elkington and G. Curthoys, J. Colloid Interface Sci., 28 (1968) 331.

[38] A.V. Kiselev and V.I. Lygin, Infrared Spectra of Surface Compounds, Wiley, New York, 1975.

[39] G. Curthoys, V.Ya. Davydov, A.V. Kiselev, et al., J. Colloid Interface Sci., 48 (1974) 58.

[40] Z. Grauer, H. Peled, D. Avnir, et al., J. Colloid Interface Sci., 111 (1986) 261.

[41] J. Jednacak-Biscan and V. Pravdic, J. Colloid Interface Sci., 75 (1980) 322.

[42] R.F. Conley and A.C. Althoff, J. Colloid Interface Sci., 37 (1971) 186.

[43] L. Heller-Kallai and S. Yariv, J. Colloid Interface Sci., 79 (1981) 479.

[44] M.S. Camazano and M.J. Martin, Geoderma, 29 (1983) 107.

[45] E. Morillo, J.L. Perez-Rodriguez and C. Maqueda, Clay Miner., 26 (1991) 269.

[46] R.E. Talbert and O.H. Fletchall, Weeds, 13 (1965) 46.

[47] T.J. Estes and V.L. Vilker, J. Colloid Interface Sci., 133 (1989) 166.

[48] P. Fruhstorfer, R.J. Schneider, L. Weil and R. Niessner, Sci. Total Environ., 138 (1993) 317.

[49] M. Cruz, J.L. White and J.D. Russell, Israel J. Chem., 6 (1968) 315.

[50] S. Tahoun and M.M. Mortland, Soil Sci., 102 (1966) 248.

[51] J.D. Russell, M.I. Cruz, J.L. White, Clay Clays Miner., 16 (1968) 21.

[52] D.A. Laird, E. Barriuso, R.H. Dowdy and W.C. Koskinen, Soil Sci. Soc. Am. J., 56 (1992) 62.

[53] R.F. Conley and M.K. Lloyd, Clays Clay Miner., 19 (1971) 273.

[54] D.P. Siantar, B.A. Feinberg, and J.J. Fripiat, Clays Clay Miner., 42 (1994) 187.

[55] M. Raupach, J. Colloid Interface Sci., 121 (1988) 466.

[56] A.G. Bezus, A.V. Kiselev, A.A. Lopatkin and P.Q. Du, J. Chem. Soc., Faraday Trans. II, 74 (1978) 367.

[57] A.A. Golub, A.I. Zubenko and B.V. Zhmud, J. Colloid Interface Sci., 179 (1996) 482.

[58] A.A. Lopatkin, Theoretical Foundations of Physical Adsorption, Moscow University Press, Moscow, 1983.

Table 1. Characteristics of the Hydrogen Bonds between Water and Polar Groups at the Surface of Silica and Layer Silicates

Bond Type	1	2	3
$-\Delta H_f$ kcal mol^{-1}	unstable	3.4/3.8[a]	6.4/2.3
d(X...H), A	-	2.57/1.84	2.20/1.84
∠(X...H-O), deg	-	141.9/162.6	144.3/167.0

[a] The first result is obtained by AM1 method, and the second by PM3-MNDO.

Table 2. Characteristics of the Hydrogen Bonds between Water and Polar Groups of Flutriafol

Bond Type	1	2	3	4
$-\Delta H_f$ kcal mol^{-1}	2.7/2.5[a]	3.8[b]/1.3	8.5/4.1	3.3/2.7
d(X...H), A	2.72/1.84	3.08[b]/1.87	2.13/1.82	2.33/1.78
∠(X...H-O), deg	112.0/177.4	87.2[b]/172.1	144.6/167.2	101.6/165.2

[a] The first result is obtained by AM1 method, and the second by PM3-MNDO.

[b] In this case, the position of water molecule is geometrically more appropriate for hydrogen bonding through the oxygen atom of the adjacent hydroxyl group of flutriafol (d(O...H) = 2.19 A, ∠(O...H-O) = 106.8°) than for bonding through the 2-nitrogen atom of the triazole group.

Table 3. Characteristics of the Hydrogen Bonds between Surface Silanols and Polar Groups of Flutriafol

Bond Type	1	2	3	4
$-\Delta H_f$ kcal mol^{-1}	3.2/0.9[(a)]	3.9/2.5	3.7/2.4	4.9/1.0
d(X...H), A	2.59/1.85	2.68/1.87	2.19/1.85	2.30/1.79
∠(X...H-O), deg	151.7/177.3	110.0/160.1	110.6/134.9	141.1/165.8

[(a)] The first result is obtained by AM1 method, and the second by PM3-MNDO.

Table 4. Parameters Used in Calculation of the Potential Energy Curves in Fig. 7.

Charge on the atoms, a.u.	Si	+1.85
	O	- 0.99
	Al	+1.95
	H	+0.24
Polarizability tensor, A^3	α_{xx}	16.2
	α_{yy}	24.1
	α_{zz}	29.8
Dipole moment, Debye	p	3.68
Intensity parameter, kcal mol^{-1}	ζ	0.05
Width parameter, A	κ	3.80

Captions

Fig. 1. Isotherms of adsorption of flutriafol. The corresponding Henry constants, Γ, are as follows: $1.7 \cdot 10^{-7}$ m (kaolinite), $8.6 \cdot 10^{-8}$ m (montmorillonite), and $2.9 \cdot 10^{-8}$ m (silica gel).

Fig. 2. Diffusion-controlled kinetics of adsorption of flutriafol. The effective diffusion coefficients are as follows: $6.5 \cdot 10^{-11}$ $m^2 s^{-1}$ (kaolinite, $\lambda = 0.75$), $3.2 \cdot 10^{-12}$ $m^2 s^{-1}$ (montmorillonite, $\lambda = 0.86$), and $5.5 \cdot 10^{-12}$ $m^2 s^{-1}$ (silica gel, $\lambda = 0.81$).

Fig. 3. Molecular mechanic model of the flutriafol-montmorillonite intercalate with the interlayer spacing of 17 A. Here, flutriafol is coordinated (dotted line) to a hydrated exchangable cation of magnesium.

Fig. 4. (a) Possible types of hydrogen bonds responsible for hydration of the surface; (b) the montmorillonite cluster used for simulation of the surface in semiempirical calculations; (c) to the explanation of instability of the type 1 hydrogen bonds.

Fig. 5. Hydrogen bond between the triazole group of flutriafol and a bridge hydroxyl group. Sterical hindrances have been artificially removed. The calculated characteristics of the bond are as follows: (AM1) $-\Delta H_f = 39.3$ kcal mol^{-1}, d(N...H) = 1.29 A, $\angle$(O-H...N) = 179.4°; (PM3-MNDO) $-\Delta H_f = 12.6$ kcal mol^{-1}, d(N...H) = 1.97 A, $\angle$(O-H...N) = 168.6°.

Fig. 6. Molecular dynamics simulation of entrance of a flutriafol molecule to the interlayer space of the montmorillonite cluster. The interlayer spacing is (°) 15 A; (•) 17 A. In each case, approximately 6000 points have been generated.

Fig. 7. Physical interaction of flutriafol with the basal plane and the edge of the montmorillonite cluster (interlayer spacing 15 A): (———) and (- - - -) the van der Waals interaction, and (- · - · -) and (· · · · ·) the electrostatic interaction.

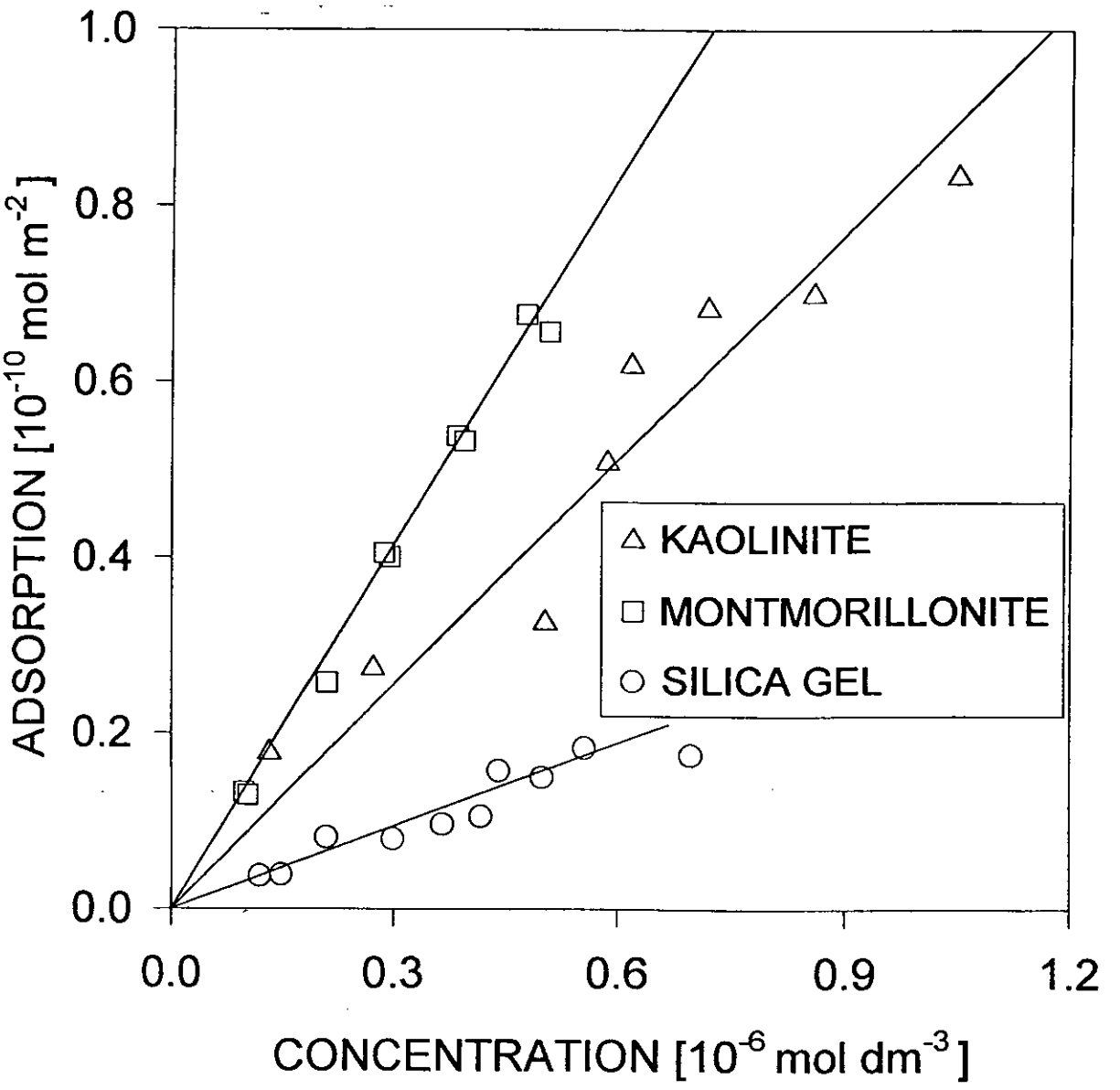
1.0
0.8
0.6
0.4
0.2
0.0
ADSORPTION [10-10 mol m-2]
0.0
0.3
0.6
0.9
1.2
CONCENTRATION [10-6 mol dm-3]
KAOLINITE
MONTMORILLONITE
SILICA GEL

Fig. 1

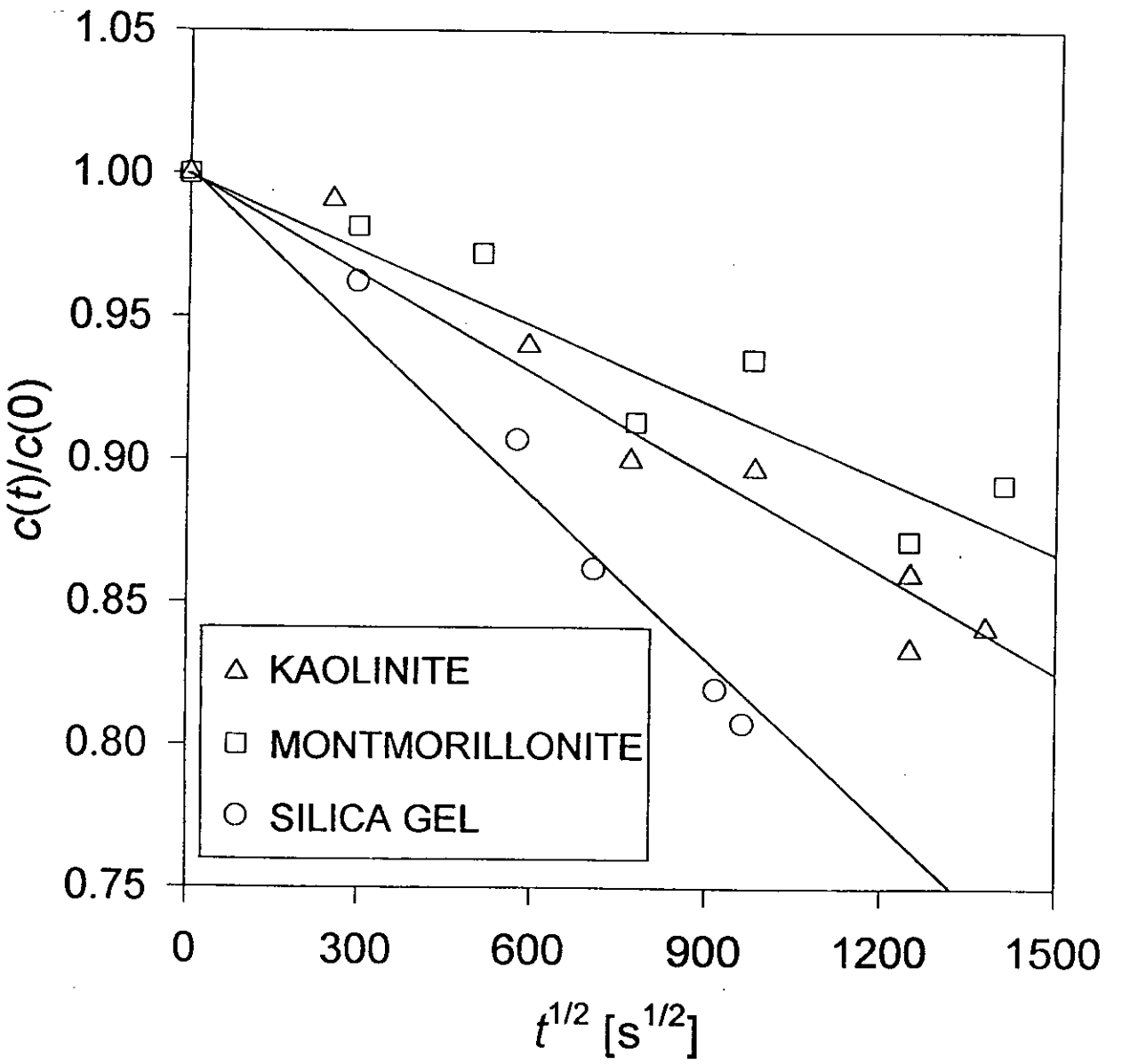
1.05
1.00
0.95
0.90
0.85
0.80
0.75
c(t)/c(0)
KAOLINITE
MONTMORILLONITE
SILICA GEL
0
300
600
900
1200
1500
t^1/2 [s^1/2]

Fig. 2

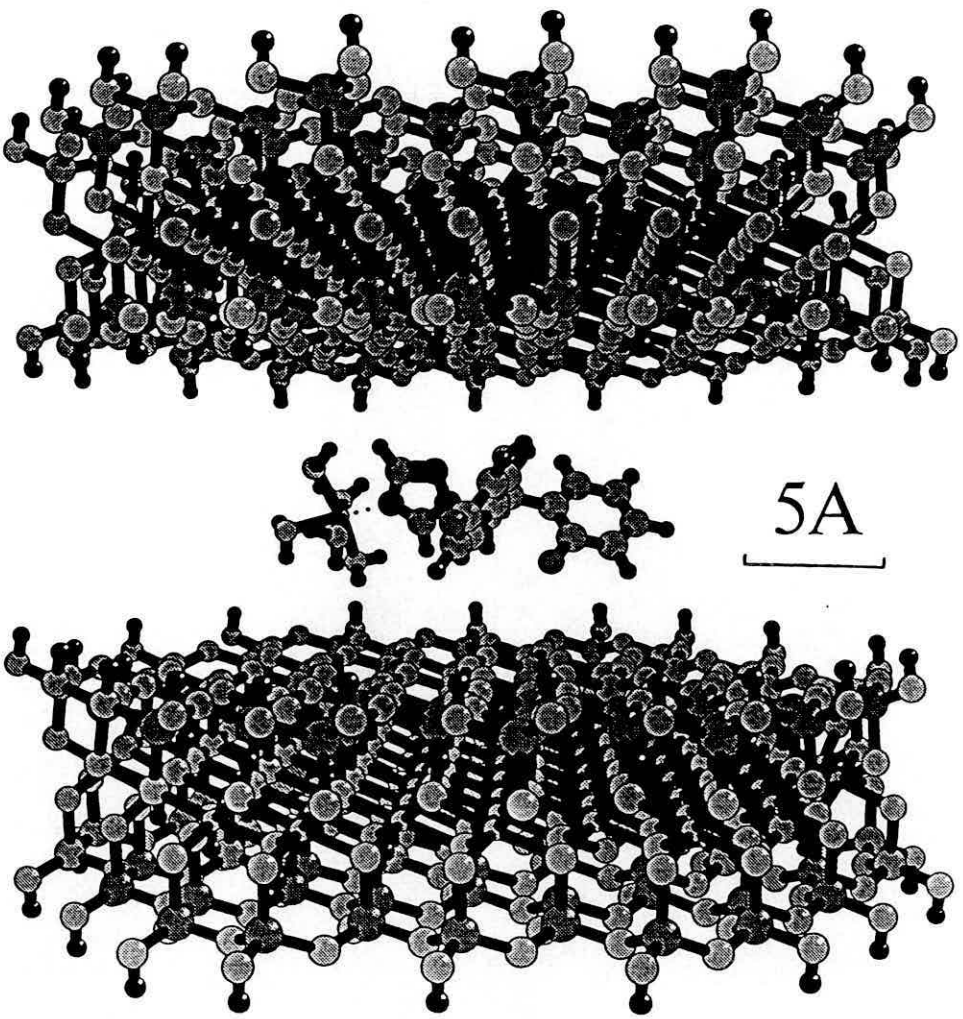

Fig. 3

Type 1

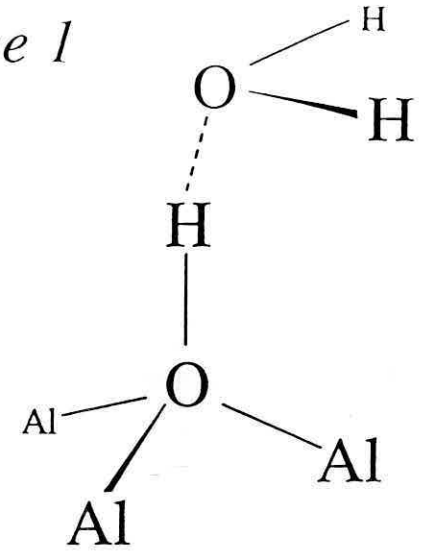

Type 2

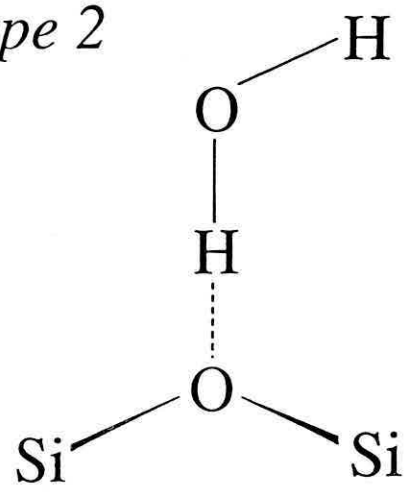

Type 3

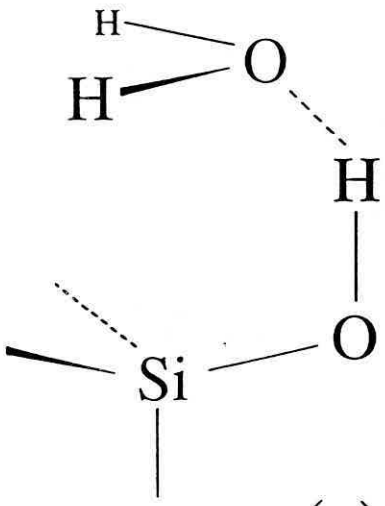

(a)

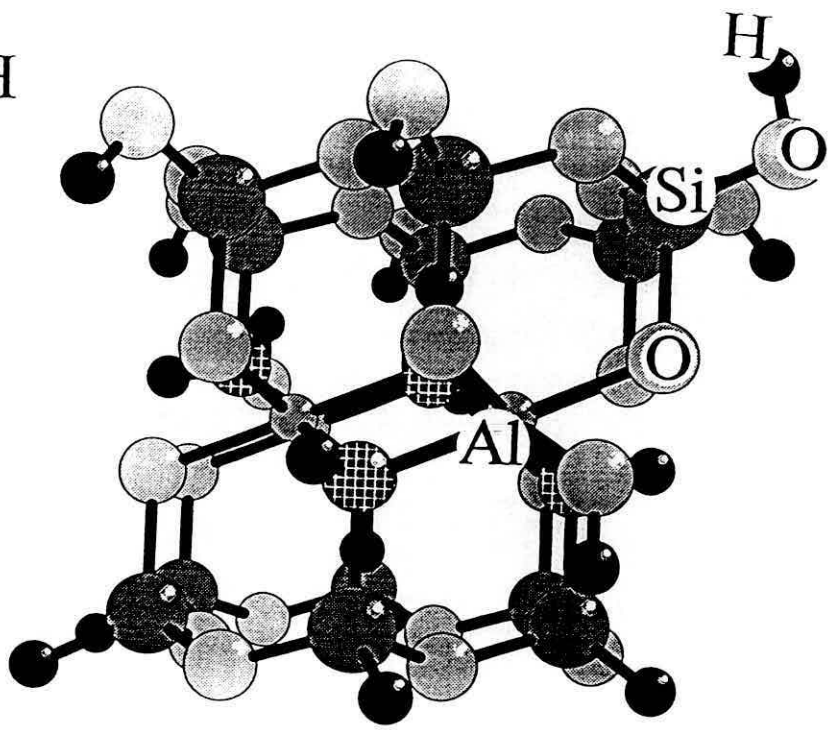

Cluster $Si_{12}O_{34}Al_4H_{14}$

(b)

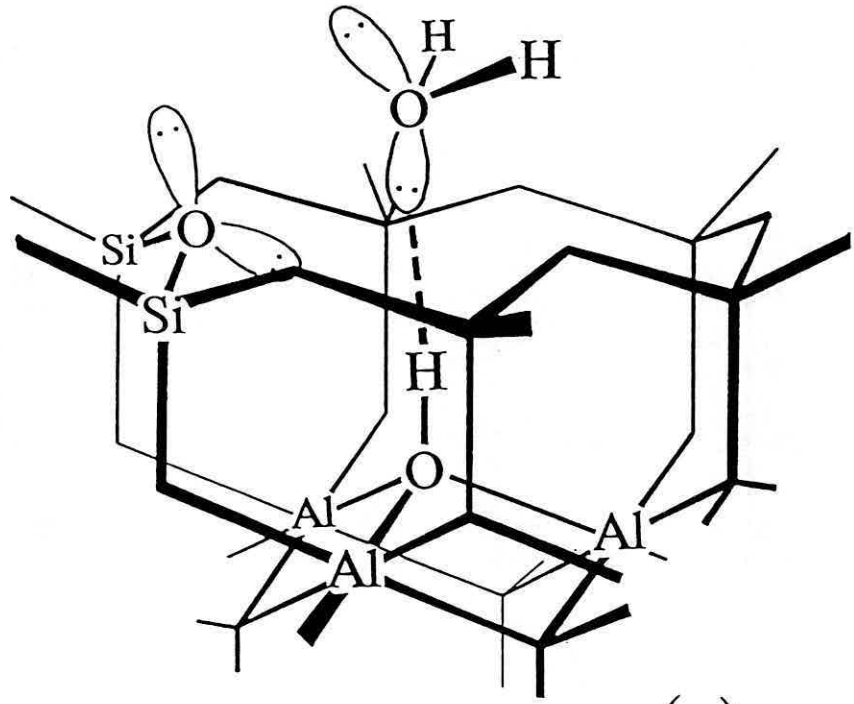

(c)

Fig. 4

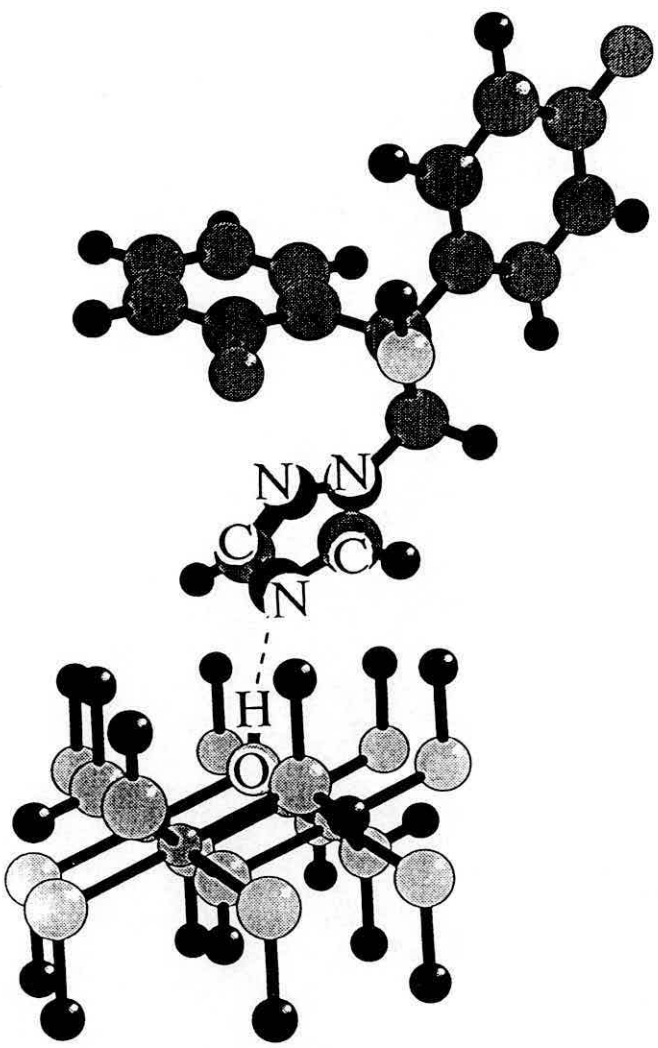

Fig. 5

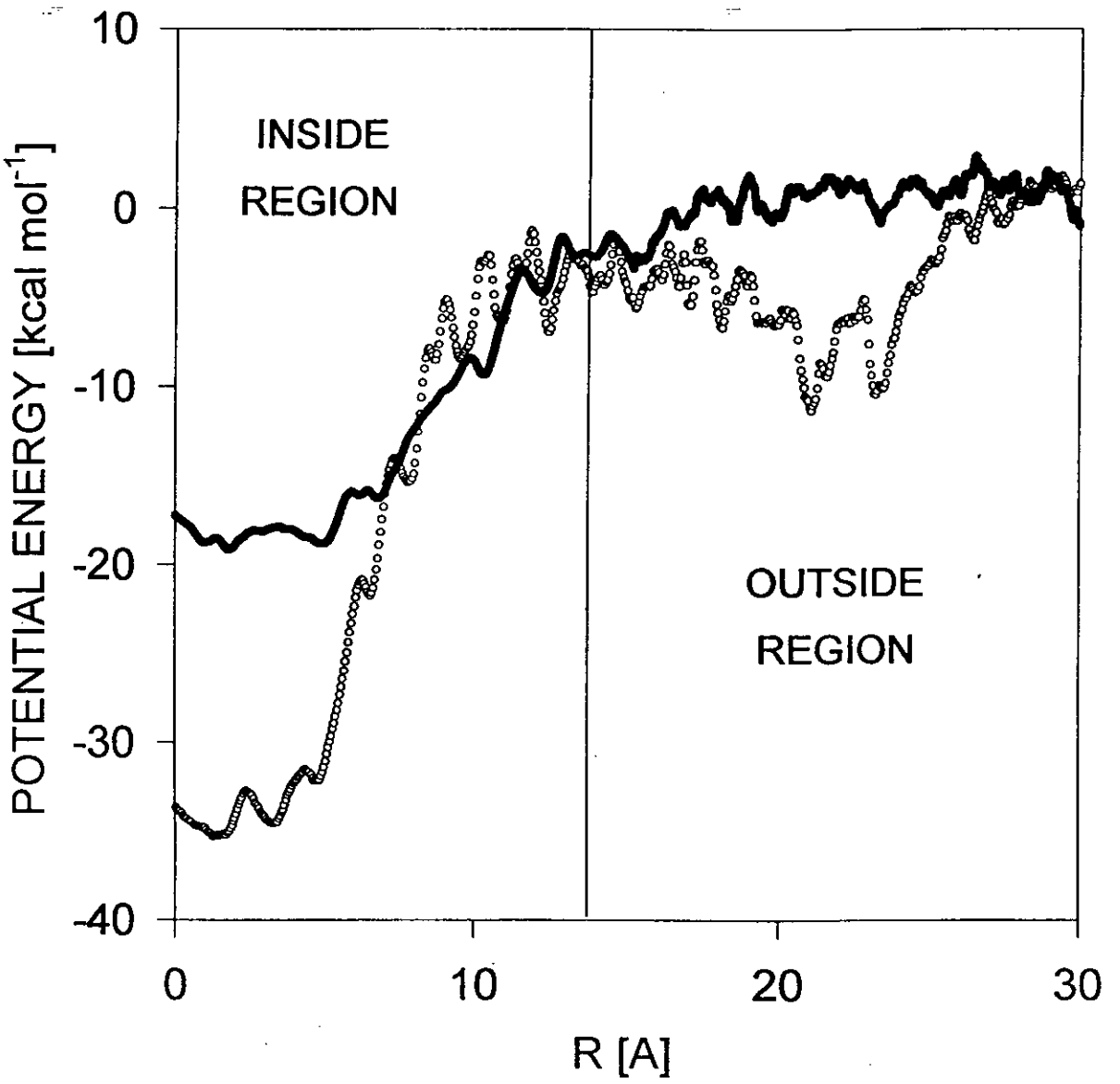
10
0
-10
-20
-30
-40
POTENTIAL ENERGY [kcal mol-1]
INSIDE
REGION
OUTSIDE
REGION
0
10
20
30
R [A]

Fig. 6

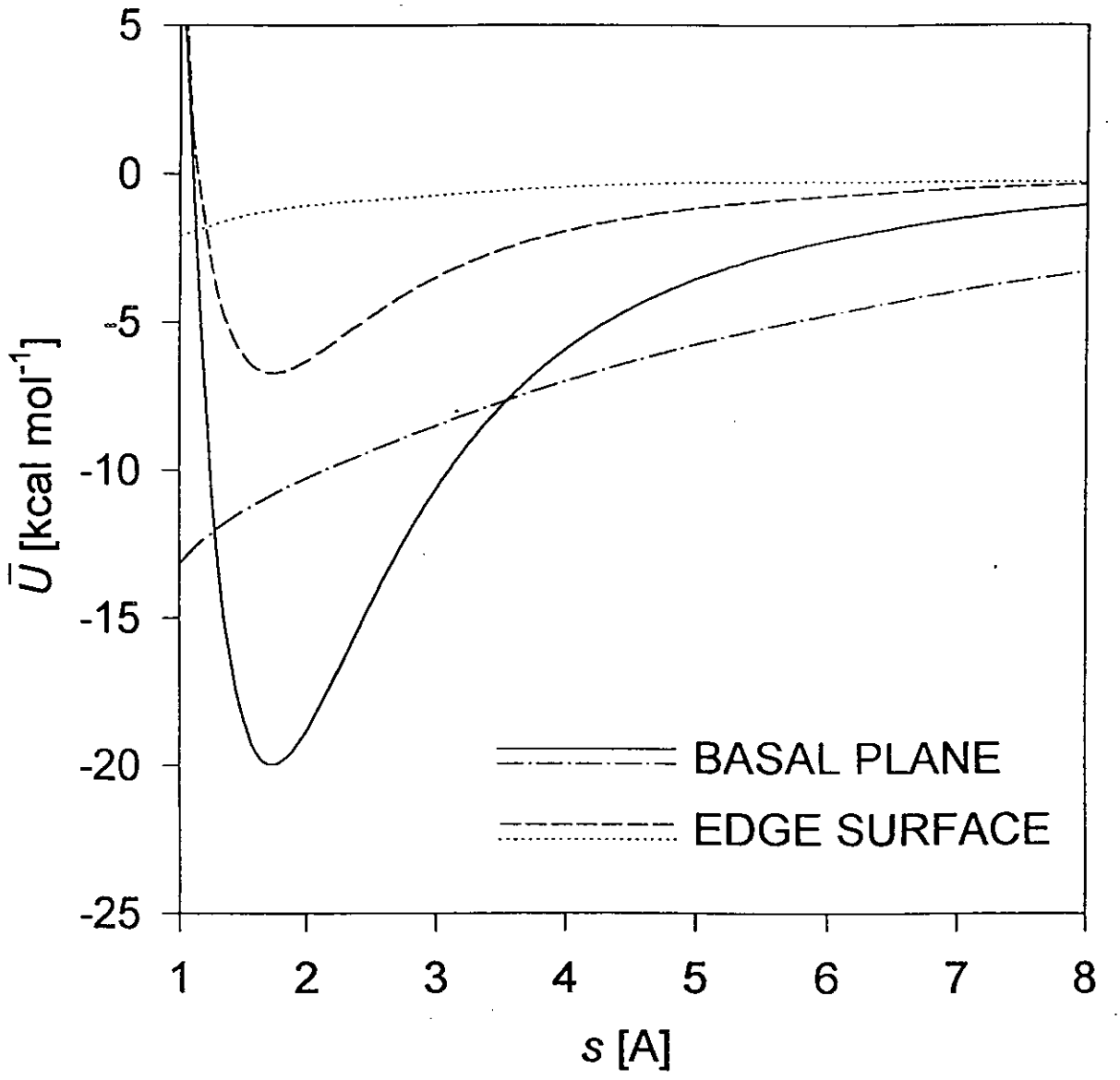
5
0
-5
-10
-15
-20
-25
$\bar{U}$ [kcal mol^{-1}]
1
2
3
4
5
6
7
8
s [A]
BASAL PLANE
EDGE SURFACE

Fig. 7


Natural
Environment
Research
Council